

Original Article

Cite this article: Parolari M, Martini M, Gómez-Tuena A, Ortega-Gutiérrez F, Errázuriz-Henao C, and Cavazos-Tovar JG (2022) The petrogenesis of Early–Middle Jurassic magmatism in southern and central Mexico and its role during the break-up of Western Pangaea. *Geological Magazine* **159**: 873–892. <https://doi.org/10.1017/S0016756822000061>

Received: 14 May 2021

Revised: 21 December 2021

Accepted: 24 January 2022

First published online: 21 February 2022

Keywords:


Mexican continental margin; Nazas igneous province; syn-rift Jurassic magmatism; Pangaea break-up; subduction initiation

Author for correspondence:

Mattia Parolari,

Email: mattiap@geologia.unam.mx

The petrogenesis of Early–Middle Jurassic magmatism in southern and central Mexico and its role during the break-up of Western Pangaea

Mattia Parolari¹ , Michelangelo Martini¹, Arturo Gómez-Tuena², Fernando Ortega-Gutiérrez¹, Carlos Errázuriz-Henao² and José G. Cavazos-Tovar²

¹Instituto de Geología, Universidad Nacional Autónoma de México, Ciudad Universitaria 04510, Mexico City, Mexico and ²Centro de Geociencias, Universidad Nacional Autónoma de México, Querétaro 76230, Mexico

Abstract

Central and southern Mexico represents a strategic place to understand the dynamics of Pangaea break-up and its influences on the evolution of the Pacific margin of North America. Lower–Middle Jurassic volcano-sedimentary successions, and scarce magmatic rocks, crop out discontinuously across this region and have been interpreted either as a vestige of a continental arc or as several deposits of syn-rift magmatism. At present, their origin is controversial. Available geochemical data on these igneous rocks suggest that they represent almost pure crustal melts produced in a rift environment rather than in an arc. In fact, the studied rocks exhibit the high silica contents and moderate to strong peraluminous character typical of sediment melts. The enriched isotopic composition (high $^{86}\text{Sr}/^{87}\text{Sr}$ and low $^{143}\text{Nd}/^{144}\text{Nd}$) and the age distributions of inherited zircon grains readily identify the widespread Upper Triassic metasedimentary sequences presently exposed in southwestern and central Mexico as the most likely crustal source of these Jurassic igneous rocks. Accordingly, we argue that these Early–Middle Jurassic magmas originated in a syn-rift igneous province associated with extensional-driven crustal attenuation in the context of Pangaea fragmentation. Our findings also constrain post-Pangaea subduction initiation to be younger than Middle Jurassic time in central and southern Mexico.

1. Introduction

The modern Pacific margin of North America extends for ~8000 km, from Alaska to Mexico, and is one of the best natural laboratories to study the range of interactions between oceanic and continental plates because of the different tectonic settings that exist along its strike (e.g. Dickinson, 2009). The Alaskan subduction zone changes southward the Queen Charlotte transform fault (Fig. 1), which is connected to the south with the Cascadia subduction zone. Further south, subduction is truncated by the San Andreas transform fault and the Gulf of California rift system, which is connected to the Acapulco trench in southern Mexico. Such discontinuities in the lateral extension of the trench are manifest by the development of a disjointed North American volcanic arc consisting of the Aleutian–Alaskan (e.g. Kay & Kay, 1988) and Cascades (e.g. O'Hara *et al.* 2020) arcs, as well as the Trans-Mexican Volcanic Belt (TMVB; Gómez-Tuena *et al.* 2018b; Fig. 1). The complex architecture of the North American Pacific margin is mainly the result of its along-strike variations relative to the convergence vector between the North America and Pacific plates. In effect, the orientation of the latter is highly variable along the North American continental edge (Fig. 1) because of the Pacific–Farallon mid-ocean ridge oblique subduction of the past ~30 Ma (Dickinson, 2009; Müller *et al.* 2019). Considering the likely variability of past convergence vectors (Müller *et al.* 2019), and that subduction of ocean and aseismic ridges likely occurred repeatedly throughout geological history (Pilger, 1981; Kinoshita, 2002; Sisson *et al.* 2003; Schoonmaker & Kidd, 2006), it seems plausible to assume that many ancient continental margins, including the North American Pacific margin itself, displayed at times a segmented configuration similar to the present one (Fig. 1). However, in most Mesozoic tectonic reconstructions, the Pacific continental edge of North America is envisioned as a continuous convergent margin, along which ongoing subduction occurred for more than ~150 Ma, between Triassic and Late Cretaceous times (Dickinson & Lawton, 2001; Pindell & Kennan, 2009; Riel *et al.* 2018). Continuous subduction beneath North America during Mesozoic time should have resulted in the development of a Triassic–Cretaceous arc along its western continental margin. Yet, available geochronological and geochemical data indicate that the central and southern segments of the Mexican Pacific margin were characterized by the absence of an active subduction zone during most of the Triassic period (Kirsch *et al.* 2014; Centeno-García, 2017; Coombs *et al.* 2020). Moreover, Early and Middle Jurassic igneous rocks in southern and central

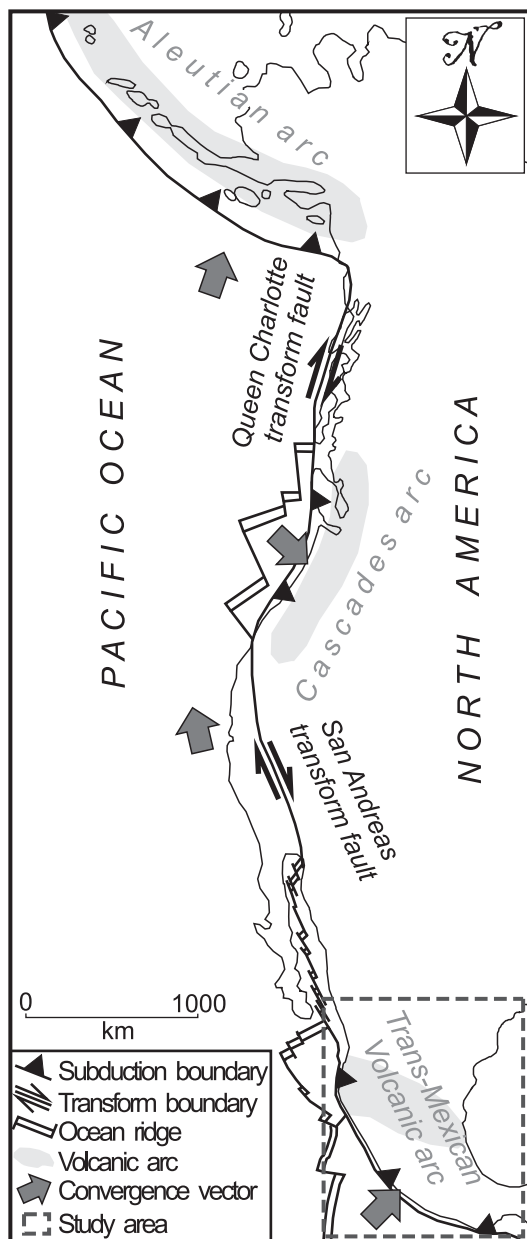


Fig. 1. Modern geotectonic configuration of the North America Pacific margins.

Mexico (Barboza-Gudiño *et al.* 2021) have been tentatively interpreted either as the vestiges of a continental arc (C. Bartolini, unpub. Ph.D. thesis, Univ. Texas at El Paso, 1998; Lawton & Molina Garza, 2014; Barboza-Gudiño *et al.* 2021) or a syn-rift igneous province associated with Pangaea break-up (Martini & Ortega-Gutiérrez, 2018; Cavazos-Tovar *et al.* 2020). A rift setting for these Jurassic rocks would imply that, contrary to what is predicted by most previous reconstructions, there would be no solid evidence of subduction beneath the central and southern segments of the Mexican Pacific margin during a large part of Triassic and Jurassic time. Based on this premise, clarifying the genesis of Jurassic igneous rocks in southern and central Mexico is key to reconstructing the evolution of the southern North American Pacific margin and understanding the processes that shaped it during early Mesozoic time.

This work reviews the available geochemical data from Early–Middle Jurassic igneous and meta-igneous rocks exposed in

southern and central Mexico, to discuss their petrogenesis and test the proposed arc and rift scenarios. After this assessment, we present a new tectonic model describing the evolution of the central and southern segments of the Mexican margin during Early–Middle Jurassic time, and further propose a new hypothesis regarding the onset of subduction in southern Mexico at the end of Jurassic time.

2. Geological background

2.a. Middle–Late Triassic time: the onset of Pangaea break-up

The fragmentation of Pangaea started by Middle–Late Triassic time with the development of a NE–SW-trending rift belt that roughly follows the Ouachita–Marathon–Sonora, Alleghanian and Variscan orogenic belts that formed during Pangaea amalgamation (Bird & Burke, 2006; Fig. 2a). During this early stage of Pangaea break-up, rift basins were infilled by voluminous, Middle–Upper Triassic fluvial to shallow-marine successions that are locally interbedded with and cut by syn-rift volcanic and intrusive rocks (Klitgord *et al.* 1988; Le Roy & Piqué, 2001; Schlische, 2003; Martin-Rojas *et al.* 2009; Frederick *et al.* 2020; Erlich & Pindell, 2021; Fig. 2b). At the same time, the development of continental arc and back-arc assemblages in the Colombian and Venezuelan Andes (Correa-Martínez *et al.* 2016; van der Lelij *et al.* 2016; Spikings & Paul, 2019), as well as in southwestern USA and northwestern Mexico (Riggs *et al.* 2013, 2016; Lawton *et al.* 2018) indicates that subduction was taking place at least beneath some parts of the western Pangaeian margin (Fig. 2b). Middle–Upper Triassic arc successions are, however, lacking in central and southern Mexico. Instead, this sector of the Pangaeian margin was the site of deposition of turbidite successions (Zacatecas, Taray, Charcas and La Ballena formations, and the Arteaga and El Chilar complexes; Centeno-García, 2005; Ortega-Flores *et al.* 2016, 2020, 2021), which have been interpreted as the stratigraphic record of submarine fans (i.e. the Potosí and Tolimán) that were deposited along the continental margin of western equatorial Pangaea and the adjacent Farallon oceanic plate (Silva-Romo *et al.* 2000, 2015; Barboza-Gudiño *et al.* 2010; Ortega-Flores *et al.* 2021; Fig. 2b). Previous studies pointed out that the youngest detrital zircon U–Pb age populations (~270–245 Ma) in these Triassic successions are considerably older (~30–10 m.y.) than the depositional age of the hosting deposits (Barboza-Gudiño *et al.* 2010; Ortega-Flores *et al.* 2014). Based on this evidence, Centeno-García (2017) suggested that the Triassic submarine fan successions were emplaced in the absence of an active magmatic arc. Even though a few subordinate detrital zircon grains of Late Triassic age have been documented in some samples from the Upper Triassic metasedimentary succession (e.g. Barboza-Gudiño *et al.* 2010; Ortega-Flores *et al.* 2021), the lack of widespread Late Triassic igneous rock exposures likely indicates that these zircons are far-travelled grains derived from distant sources in northwestern Mexico and northwestern South America. Likewise, the minor occurrence of Late Triassic zircon grains in modern fluvial and littoral deposits draining a large sector of southern Mexico (Cavazos-Tovar *et al.* 2020) documents a clear gap in magmatism and zircon production, and supports the lack of a Late Triassic arc, at least along this sector of the western Pangaeian margin.

Based on the increasing evidence of the lack of a magmatic arc, Centeno-García (2017) proposed that the central and southern

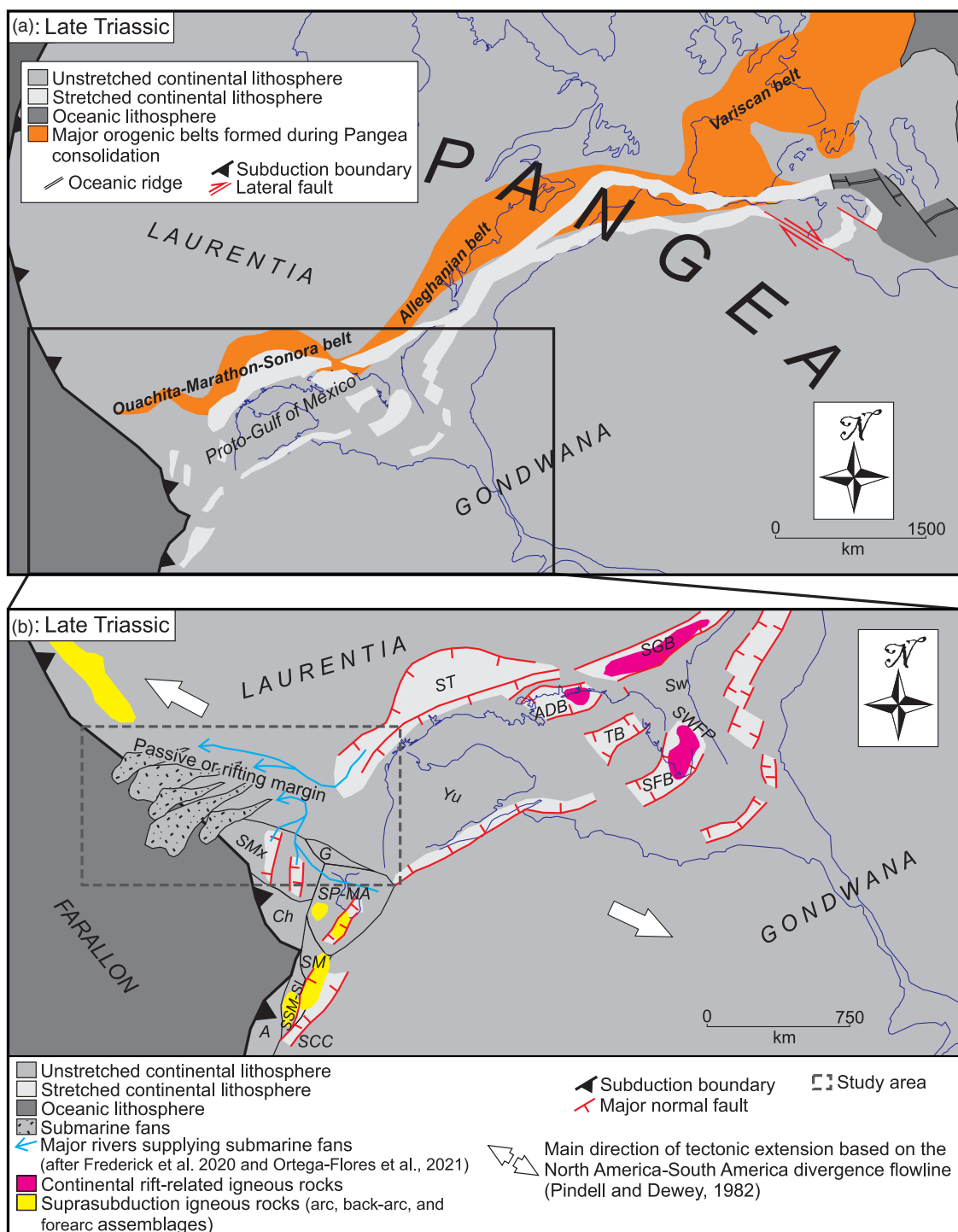


Fig. 2. (Colour online) (a) Reconstruction of the supercontinent Pangaea in Late Triassic time (~230–210 Ma). The reconstruction is obtained by integrating previous reconstructions and data published by Dickinson & Lawton (2001), Le Roy & Piqué (2001), Schettino & Turco, (2009), Labails *et al.* (2010) and Pindell *et al.* (2021). (b) Geotectonic reconstruction of the western equatorial margin of Pangaea in Late Triassic time (~230–210 Ma). The reconstruction shows the areas that experienced continental attenuation and the distribution of subduction-related and continental rift-related igneous rocks. The reconstruction of the Florida and Yucatán areas is based on data presented in Erlich & Pindell (2021) and Frederick *et al.* (2020). The Mexican sector of the Pangaeian margin is reconstructed according to data in Pindell *et al.* (2021) and Ortega-Flores *et al.* (2021). The Colombian sector of the Pangaeian margin is according to Bayona *et al.* (2010), van der Lelij *et al.* (2016), Bayona *et al.* (2020) and Spikings & Paul (2019). A – Antioquia block; ADB – Apalachicola–Desoto Canyon Basin; Ch – Chortis block; G – Guajira block; SP-MA – Merida Andes–Sierra de Perijá block; SCC – Southern Central Cordillera of Colombia; SFB – South Florida Basin; SGB – South Georgia Basin; SM – Santander Massif block; SMx – South Mexico block; SSM-SL – Sierra de Santa Marta–San Lucas block; ST – South Texas Basin; Sw – Swannee terrane; SWFP – Southwest Florida Mesozoic volcanic province; TB – Tampa Basin; Yu: Yucatán block.

Mexican sector was a passive or rifted margin during Late Triassic time (Fig. 2b). The juxtaposition of this Late Triassic passive or rifted margin with the adjacent convergent boundaries to the north

and south requires the existence of major transform faults dissecting the western equatorial margin of Pangaea. However, none of these Late Triassic faults have been documented and no

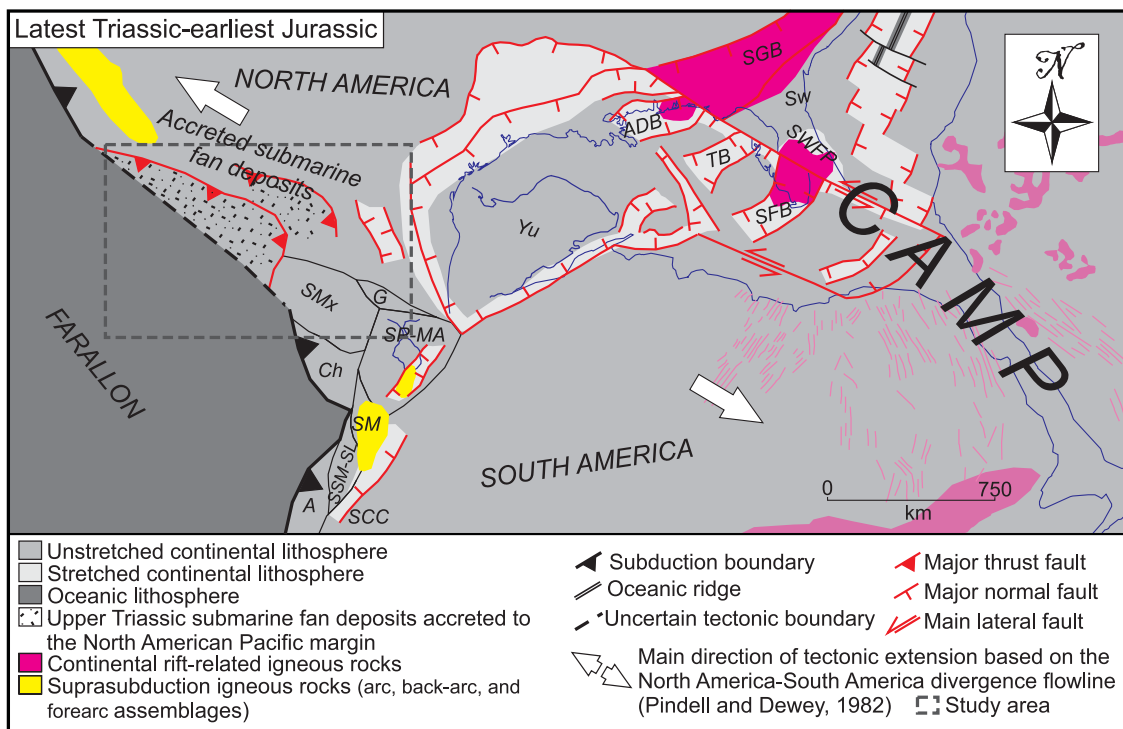


Fig. 3. (Colour online) Geotectonic reconstruction of the North America – South America divergent boundary between latest Triassic and earliest Jurassic time (~202–200 Ma; based on Boschman *et al.* 2014; Marzoli *et al.* 2018; Bayona *et al.* 2020; Erlich & Pindell, 2021 and Pindell *et al.* 2021). The reconstruction shows the areas that experienced continental attenuation and the major normal to lateral faults that accommodated divergence between North and South America. It also shows the extension of the Central Atlantic Magmatic Province (CAMP) associated with the continental rifting, as well as the distribution of the subduction-related magmatism along the Pacific margins of the Americas. A – Antioquia block; ADB – Apalachicola–Desoto Canyon Basin; Ch – Chortis block; G – Guajira block; SP-MA – Merida Andes–Sierra de Perijá block; SCC – Southern Central Cordillera of Colombia; SFB – South Florida Basin; SGB – South Georgia Basin; SM – Santander Massif block; SSM-SL – Sierra de Santa Marta–San Lucas block; ST – South Texas Basin; Sw – Swannee terrane; SWFP – Southwest Florida Mesozoic volcanic province; TB – Tampa Basin; Yu – Yucatán block.

indirect evidence has yet been identified. Moreover, the conjugate for the Mexican rifted margin has not been found, making the passive-rifting margin scenario speculative. In contrast, Vega-Granillo *et al.* (2020) recently proposed a model in which the Upper Triassic metasedimentary successions of southern and central Mexico were developed in a more complex tectonic setting, in which an ENE-elongated continental rift basin, roughly separating southern and northern Mexico, interacted with a major subduction boundary that developed along the western margin of Pangaea. However, this scenario requires the development of a Late Triassic extensional arc in southern and central Mexico and, thus, is not supported by available geochronological data that document a gap in the magmatic activity during Late Triassic time. Between Late Triassic and earliest Jurassic times, the submarine fan deposits were folded, sheared and tectonically transported to the NE (Ortega-Flores *et al.* 2016; Vázquez-Serrano *et al.* 2019; Fig. 3). Shortening of the Triassic succession produced an orogenic wedge (Vázquez-Serrano *et al.* 2019) that presently extends from the trench into the continental interior, with the easternmost exposures almost bounding the western Gulf of Mexico (GM). The total thickness of this orogenic wedge is unknown, although a minimum thickness of ~7 km is depicted in structural sections by some authors (e.g. Vázquez-Serrano *et al.* 2019). The dynamics and the driving forces of this deformation event are not yet understood. Some authors speculated that shortening of the Upper Triassic submarine deposits was linked to the onset of eastward subduction beneath the North American Pacific margin, or to the westward subduction beneath an exotic Pacific island arc that was subsequently accreted to the North American continental margin

(Anderson *et al.* 1990; Centeno-García & Silva-Romo, 1997; Centeno-García, 2017; Vázquez-Serrano *et al.* 2019). A few mafic rocks interpreted as exotic blocks within the sheared and folded submarine fan deposits display geochemical and isotopic signatures of island-arc tholeiites and a high pressure – low temperature paragenesis (5–7 kbar and 200–330 °C, respectively; Talavera-Mendoza, 2000). However, as the age of these metamorphic mafic rocks is unknown, the hypothesis that they are contemporaneous to the Upper Triassic successions of Mexico remains unconfirmed.

2.b. Latest Triassic – earliest Jurassic time: the emplacement of the Central Atlantic Magmatic Province and opening of the Atlantic Ocean

The Triassic–Jurassic boundary is marked by the formation of the first ocean ridge in the proto-Atlantic, between Morocco and Nova Scotia (Sahabi *et al.* 2004; Schettino & Turco, 2009; Labails *et al.* 2010; Fig. 3). This magmatism heralded the development of the Central Atlantic Magmatic Province (CAMP; Fig. 3), the most extensive magmatic province in Earth's history (Marzen *et al.* 2020), the vestiges of which are presently exposed along eastern North and South America, western Africa and southwestern Europe (e.g. Marzoli *et al.* 2018). The CAMP is dominated by basaltic rocks with ages in the range of ~202 to 192 Ma (primarily $^{40}\text{Ar}/^{39}\text{Ar}$ in plagioclase), with a peak at ~201 Ma (Marzoli *et al.* 2018). Igneous rocks of the CAMP were originally considered the magmatic manifestation of a deep-mantle plume that potentially contributed to Pangaea break-up (Morgan, 1983; Hill, 1991). However, it has been increasingly recognized that

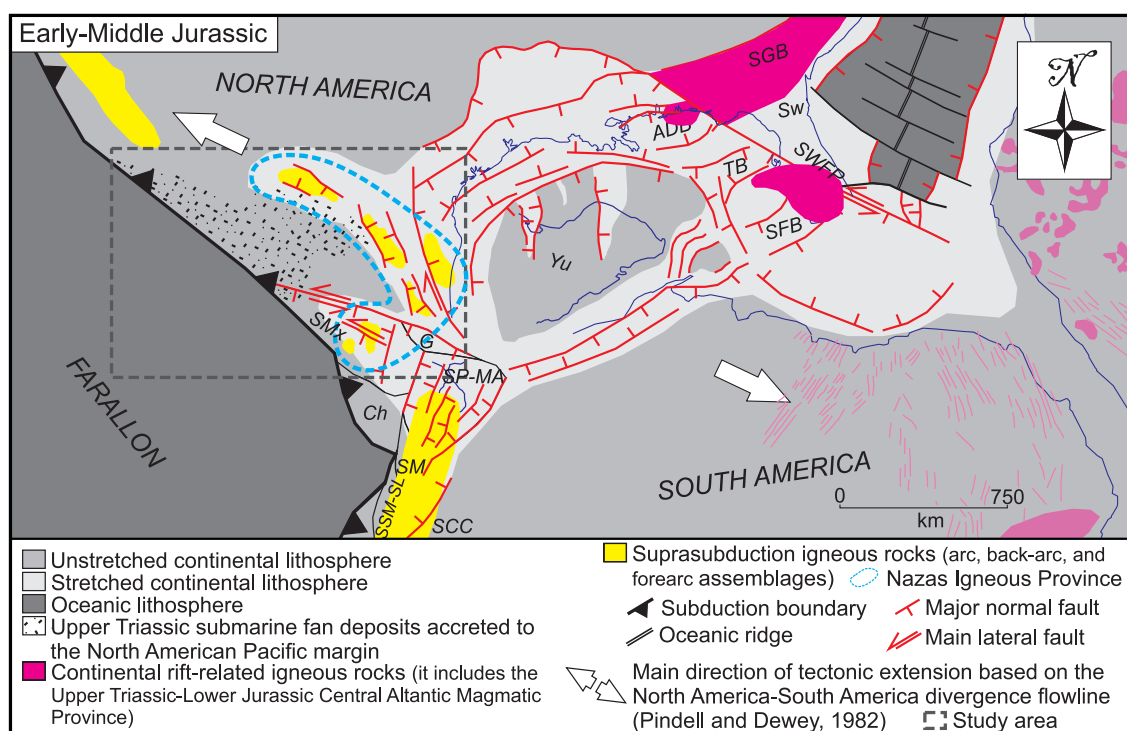


Fig. 4. (Colour online) Geotectonic reconstruction of the North America – South America divergent boundary during Early–Middle Jurassic time (~190–170 Ma); based on Boschman *et al.* 2014; Bayona *et al.* 2020; Erlich & Pindell, 2021 and Pindell *et al.* 2021). The reconstruction shows the areas that experienced continental attenuation and the distribution of subduction-related igneous rocks (including the Nazas igneous province), as well as of the continental rift-related igneous rocks. A – Antioquia block; ADP – Apalachicola–Desoto Canyon Basin; Ch – Chortis block; G – Guajira block; SP-MA – Merida Andes–Sierra de Perijá block; SCC – Southern Central Cordillera of Colombia; SFB – South Florida Basin; SGB – South Georgia Basin; SM – Santander Massif block; SMx – South Mexico block; SSM-SL – Sierra de Santa Marta–San Lucas block; ST – South Texas Basin; Sw – Swannee terrane; SWFP – Southwest Florida Mesozoic volcanic province; TB – Tampa Basin; Yu – Yucatán block.

the genesis of the CAMP is more likely related to decompression melting of shallow upper mantle during Pangaea break-up due to the moderate rise of mantle temperature that resulted from long-term heat incubation underneath the Pangaea supercontinent (Hole, 2015; Marzen *et al.* 2020), possibly related to the mantle return flow generated by the subduction of cold oceanic plates along the supercontinent's edges (Heron, 2019). The formation of such a huge thermal anomaly (the African superplume; Zhong *et al.* 2007) likely represented a response to the development and establishment of the present-day degree-2 mantle convection during the formation of the supercontinent, which in turn may have exerted a significant control on the development and migration of Cordilleran arcs during the last ~180 Ma (Spencer *et al.* 2019).

2.c. Early–Middle Jurassic time: the Nazas igneous province

The progressive break-up of Pangaea between ~195 and ~168 Ma was accommodated by normal to lateral faults with different orientations, mostly following previous zones of weakness between terranes (e.g. Erlich & Pindell, 2021; Fig. 4). Based on a multi-stage, global plate-reconstruction model of western equatorial Pangaea, Pindell *et al.* (2020) estimated continental extension in the order of 600 km and 400 km in the western and eastern proto-GM, respectively. Crustal thinning during this time interval favoured the emplacement of syn-rift basaltic, rhyolitic and minor andesitic lava flows, dykes and sills in the South Georgia rift basin (Heatherington & Mueller, 1999; Heffner *et al.* 2012), the Southwest Florida Mesozoic volcanic province (Heatherington & Mueller, 1991, 2003) and the Apalachicola and South Florida

basins (Erlich & Pindell, 2021; Fig. 4). To the west, along the northern and southern margins of the Yucatán block, Early–Middle Jurassic syn-rift igneous rocks have not been observed at the surface or reached by wells. The lack of igneous rocks has motivated many authors to suggest that extension along the northern and southern margins of the Yucatán block was essentially amagmatic (e.g. Frederick *et al.* 2020). However, magnetic and gravity anomalies suggest the existence of a deeply buried volcanic rifted margin in southern Texas (Mickus *et al.* 2009; Maus *et al.* 2009), but the age of these hypothesized volcanic rocks is unknown.

Lower–Middle Jurassic arc and back-arc assemblages are distributed in the Colombian, Venezuelan and Peruvian Andes (van der Lelij *et al.* 2016; Quandt *et al.* 2018; Bayona *et al.* 2020; López-Isaza & Zuluaga, 2020), as well as in North America across the length of southern California and western Nevada, continuing southwestward into Arizona and northwestern Mexico (Busby-Spera, 1988; Tosdal *et al.* 1989; Busby-Spera *et al.* 1990; Haxel *et al.* 2005; González-León *et al.* 2021; Fig. 4). These assemblages indicate that, during Early and Middle Jurassic time, subduction persisted at least beneath some sectors of the Pacific margin of South and North America. In central and southern Mexico, scattered exposures of Lower–Middle Jurassic volcano-sedimentary successions and rare subvolcanic and intrusive to meta-intrusive rocks are presently distributed between Torreón, Acapulco and Tuxtla Gutiérrez (C. Bartolini, unpub. Ph.D. thesis, Univ. Texas at El Paso, 1998; Campa-Uranga *et al.* 2004; Godínez-Urban *et al.* 2011; Helbig *et al.* 2012; Zavala-Monsiváis *et al.* 2021; Lawton & Molina Garza, 2014; Barboza-Gudiño *et al.* 2021; Fig. 5). The volcano-sedimentary successions are dominantly composed of fluvial deposits alternated with felsic pyroclastic rocks

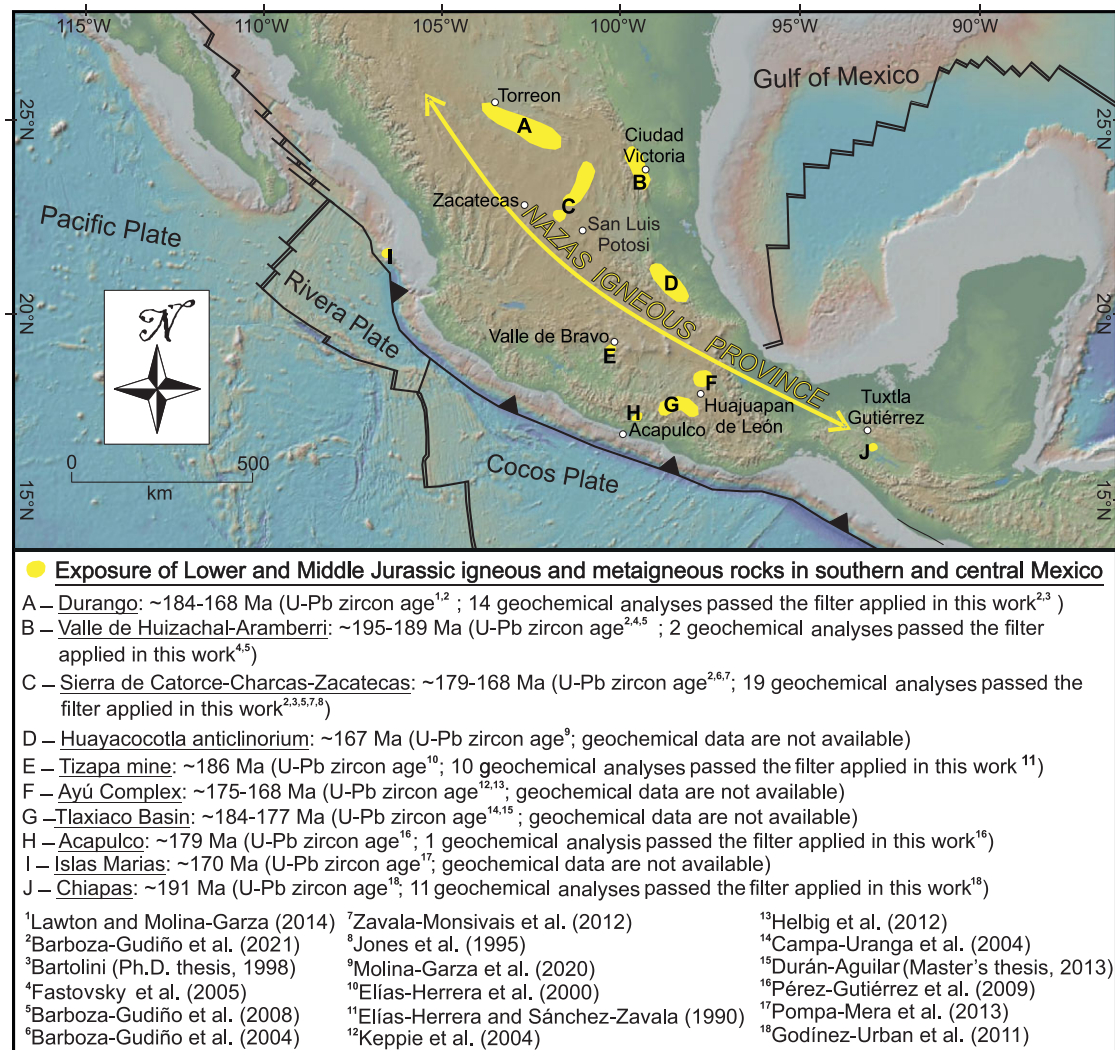


Fig. 5. (Colour online) Schematic map showing the distribution of igneous and meta-igneous rocks of Early and Middle Jurassic age in central and southern Mexico. No systematic geochemical variations are observed among data from different localities (see online Supplementary Material Fig. S1: chemical variation of NIP rocks).

and subordinate mafic to intermediate lava flows (C. Bartolini, unpub. Ph.D. thesis, Univ. Texas at El Paso, 1998; Lawton & Molina Garza, 2014). Subvolcanic and (meta)intrusive bodies are dominantly granitic in composition (López Infanzón, 1986; Elías Herrera & Sánchez Zavala, 1990; Pérez-Gutiérrez *et al.* 2009; Helbig *et al.* 2012; Pompa-Mera *et al.* 2013). Isotopic ages previously reported for these igneous rocks span from ~230 to ~70 Ma (Pb- α , Rb-Sr, K-Ar and Ar-Ar; Bartolini *et al.* 2003 and references therein). However, many of these ages contradict solid stratigraphic relationships, suggesting that, after magmatic emplacement, these rocks experienced a complex thermal history (e.g. Zavala-Monsiváis *et al.* 2012). Based on zircon U–Pb ages, almost all authors agree in bracketing the crystallization age of these rocks between ~191 and ~165 Ma (Fig. 5 and references therein). However, U–Pb ages on detrital zircon grains from Jurassic fluvial deposits show that the magmatic activity in central and southern Mexico likely spanned ~35 m.y., from ~200 to ~165 Ma (e.g. Lawton & Molina-Garza, 2014).

These Early and Middle Jurassic igneous rocks exposed in central and southern Mexico are part of the Nazas igneous province (NIP). Most authors (C. Bartolini, unpub. Ph.D. thesis, Univ. Texas at El Paso, 1998; Lawton & Molina-Garza, 2014;

Barboza-Gudiño *et al.* 2021) interpreted those rocks as the vestiges of a continental arc (hereafter referred to as the Nazas Arc), which is inferred to be the connection between the Cordilleran arc in the southwestern USA and the continental arc of South America (Fig. 4). Based on the abundance of epiclastic deposits interbedded with volcanic rocks and the evidence of progressive exhumation of basement rocks (Rubio-Cisneros & Lawton, 2011; Lawton & Molina Garza, 2014), the Nazas Arc has been interpreted as a continental extensional arc. In the last few years, however, Martini & Ortega-Gutiérrez (2018) and Cavazos-Tovar *et al.* (2020) suggested that the NIP is likely a syn-rift magmatic province that was formed as a result of crustal thinning associated with Pangaea break-up, with negligible subduction influence. This alternative scenario is based on the observation that, at least in central and southern Mexico, these Early and Middle Jurassic igneous rocks were emplaced in continental extensional to transtensional rift basins, the kinematics of which is closely linked to the NW–SE divergence between North and South America and is incompatible with a SE convergence vector along the Pacific margin of North America (Martini & Ortega-Gutiérrez, 2018). Moreover, Cavazos-Tovar *et al.* (2020) showed that the overall negative ϵ_{Hf} values and the trace-element systematics of Jurassic

zircon grains in modern fluvial and littoral deposits associated with the NIP rocks suggest melting of a metasedimentary crustal source in the genesis of these Early–Middle Jurassic magmas. At present, an exhaustive petrogenetic study of the NIP has not been completed; therefore, its origin remains controversial and the timing and mechanism of subduction initiation along the continental margin of Mexico are still under debate.

3. Methods: data treatment

In this work, we present a compilation (121 samples) of whole-rock geochemical data available from the literature for Early and Middle Jurassic igneous and meta-igneous rocks exposed in central and southern Mexico (online Supplementary Material Table S1). We selected only those samples for which the age and stratigraphic position are well known. Accordingly, we do not consider samples from igneous and meta-igneous exposures with a stratigraphic position that has been tentatively defined by some authors, successively challenged by others and presently is not yet exhaustively resolved. We also exclude from our database those samples from volcanic and metavolcanic layers for which the age has been inferred based on a poorly defined maximum depositional age (defined by fewer than three grains with concordant ages overlapping at 2σ) of the interbedded clastic deposits.

Although the amount of data published by previous authors is significant, deciphering the origin of the Early–Middle Jurassic magmatism in Mexico is challenging, primarily owing to the moderate to pervasive weathering of the igneous and meta-igneous rocks (e.g. Barboza-Gudiño *et al.* 2021). In fact, most of the compiled chemical analyses display high loss on ignition values (LOI >3 wt%; online Supplementary Material Table S1 and Fig. 6). In addition, primary mineral phases are largely replaced by secondary clay minerals, oxides and hydroxides (Fastovsky *et al.* 2005; Barboza-Gudiño *et al.* 2010; Godínez-Urban *et al.* 2011; Barboza-Gudiño *et al.* 2021). To minimize the effect of weathering on the petrogenetic interpretation, we filtered the available data by rejecting analyses characterized by high LOI values (>3 wt%) and by using a combination of weathering-related parameters that aim to increase the reliability of the selected analysis. Specifically, we consider two different weathering indexes: the Chemical Index of Alteration (CIA; Nesbitt & Young, 1982) and the Weathering (W) index (Ohta & Arai, 2007). The CIA is expressed by the ratio of immobile (i.e. Al) to major mobile elements (i.e. Na, Ca and K). Accordingly, less weathered rocks show low CIA values (c. 40–50), and higher values (up to 100) are related mainly to the formation of minerals like kaolinite and sericite at the expense of feldspars, as a result of pervasive and/or protracted weathering (Perri, 2020). The W index is a geochemical index built on a statistical analysis of major-element behaviour during weathering (Ohta & Arai, 2007). High values of the W index indicate moderate to pervasively weathered samples, whereas values in the range of 10–20 are common in fresh rocks (Perri, 2020). On a global set of data, these indices display a well-developed positive correlation (Perri, 2020) and are thus suitable to be used as complementary parameters to evaluate the weathering extent of the selected rock samples. Applied to our data compilation, the CIA and W indexes show that ~20% of the geochemical analyses available were performed on moderately to pervasively weathered samples, the composition of which is the result of extensive mobilization of soluble elements (Fig. 6). In this work, these samples (CIA >80; W index >80) were not considered as representative of the original magmatic compositions and discarded.

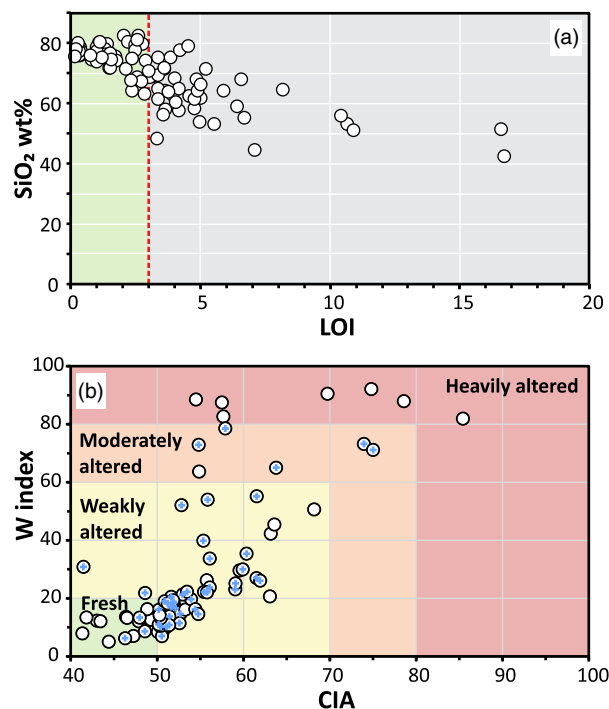


Fig. 6. (Colour online) Loss on ignition (LOI) and two different weathering indexes of the compiled chemical analysis (see online Supplementary Material Table S1 for data sources). (a) A conspicuous amount of the samples show high values of LOI and (b) moderate to high weathering conditions (alteration fields Perri, 2020). Small blue crosses in (b) represent the selected samples once the filter is applied (see Section 3 for details). CIA = Chemical Index of Alteration (Nesbitt & Young, 1982); $CIA = Al_2O_3 / (Al_2O_3 + K_2O + Na_2O + CaO) \times 100$ (molar amounts); the equations and the steps used to calculate the W index are listed in Ohta & Arai (2007).

A critical issue in interpreting the genesis of Early–Middle Jurassic igneous and meta-igneous rocks from central and southern Mexico is that most of the studied intermediate and mafic rocks display high LOI (Fig. 6a). Accordingly, in our filtered selection (57 samples), the composition of these rocks varies from rhyolite to dacite (Fig. 7a, b). However, as the number of samples that were originally classified as mafic represents only 4% of the available data, we believe that our filtered dataset offers an accurate portrait of the compositional variability of the NIP. Nonetheless, we are aware that our analysis may be biased to the filtered felsic NIP rocks, and that our conclusions may not be simply extrapolated to the altered mafic counterparts. Nonetheless, we show that a careful evaluation of the major and trace elements of the filtered samples, as well as their comparisons with other magmatic suites from well-established tectonic settings, allows us to obtain relevant information on the petrogenesis of the NIP and its potential parental mafic magmas. For the sake of simplicity, in the following discussion we will refer to the NIP rock suite as pertaining to the filtered dataset unless otherwise noted.

4. Main geochemical features of the Nazas igneous province

The NIP comprises felsic volcanic and volcanoclastic units, with minor volumes of subvolcanic, intrusive and meta-intrusive rocks of calc-alkaline affinity (C. Bartolini, unpub. Ph.D. thesis, Univ. Texas at El Paso, 1998; Campa-Uranga *et al.* 2004; Godínez-Urban *et al.* 2011; Zavala-Monsiváis *et al.* 2012; Lawton & Molina Garza, 2014; Barboza-Gudiño *et al.* 2021). These rocks

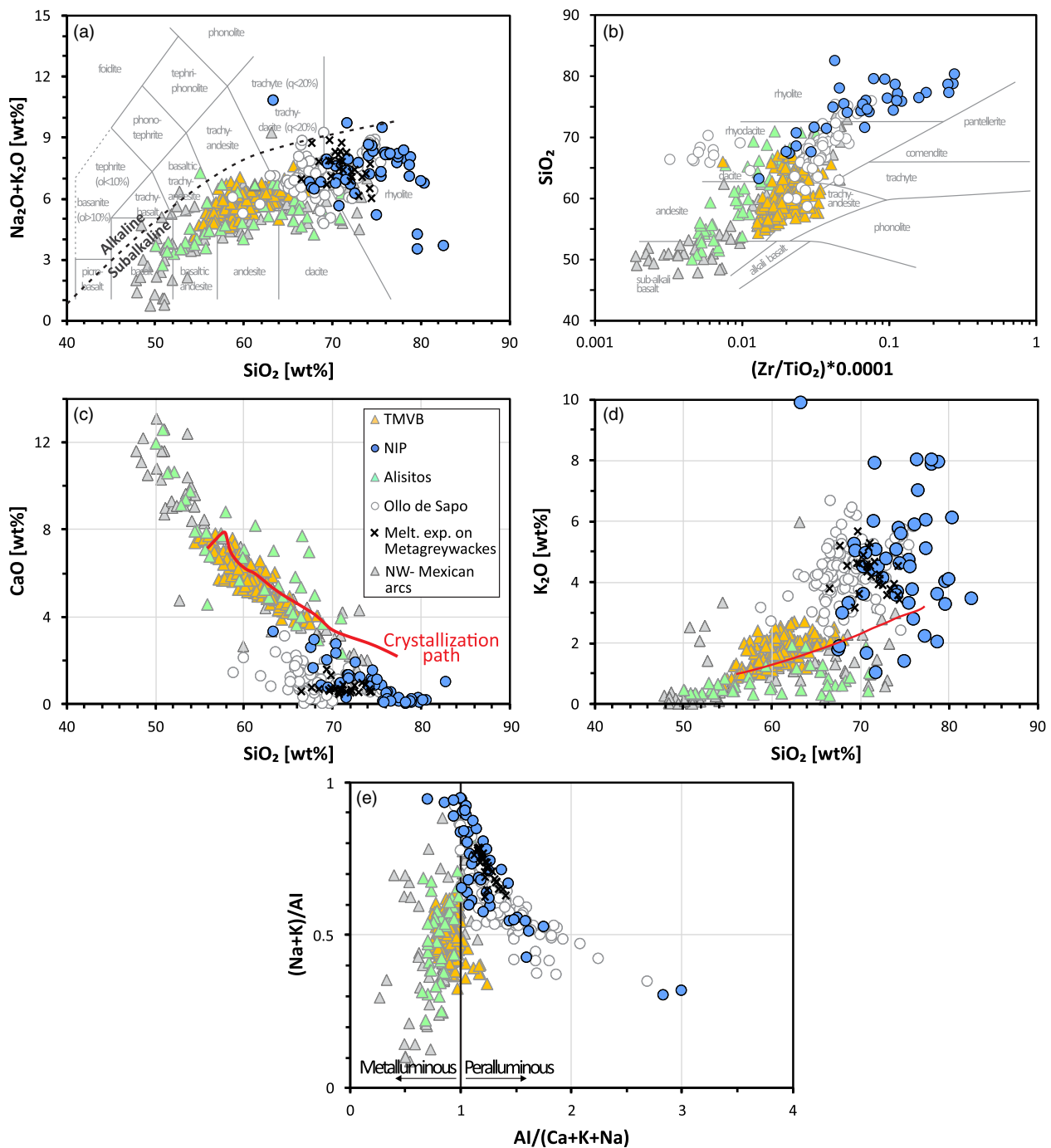


Fig. 7. (Colour online) (a) Total alkali versus silica (TAS; Bas *et al.* 1986) classification diagram and major-element compositions of the NIP rocks. Dashed line in (a) indicates the boundary between the alkaline and subalkaline fields according to Irvine & Baragar (1971). (b) Variation diagram intended for geochemical classification of altered and metamorphosed rocks (Winchester & Floyd, 1977). Red lines in (c) and (d) are fractional crystallization Rhyolite-MELTS models (Gualda *et al.* 2012) of the high Mg no. basaltic-andesite from the Popocatepetl volcano (Sample POS-9 from Straub *et al.* 2011) starting at a pressure of 10 kbar and a temperature of 1210 °C, considering a H_2O wt % of 4 and a fixed oxygen fugacity ($Q_{\text{FM}} = 1$). Accordingly, the major-element concentrations of the NIP rocks cannot be considered as the results of a process of crystal fractionation of an archetypal primitive arc magma. (e) Diagram showing the aluminium saturation index (ASI). Added for comparison are the compositions of some Mexican arc rocks (Alisitos Arc, Morris *et al.* 2019; Mexican Stratovolcanoes, Parolari *et al.* 2021; NW Mexico, Contreras-López *et al.* 2018, 2021; Torres-Carrillo *et al.* 2020); liquid compositions of a fluid-absent partial melting experiment on metagreywackes (Montel & Vielzeuf, 1997) and the Ollo de Sapo magmatic suite (García-Arias *et al.* 2018).

display a limited compositional range, with high SiO_2 (average = 74.3 wt %) and alkali contents (average $\text{Na}_2\text{O} + \text{K}_2\text{O} = 7.47$ wt %; $\text{K}_2\text{O}/\text{Na}_2\text{O} = 6.25$), low MgO and FeO (average $\text{MgO} + \text{FeO} = 3.15$ wt %), low Ca (average 0.92 wt %) and, with the exception of a few samples (5 out of 57 in our filtered dataset), moderate to strong peraluminous compositions (Fig. 7e).

According to the total alkali versus silica (TAS) diagram (Bas *et al.* 1986), and to the SiO_2 versus Zr/TiO_2 classification diagram (Winchester & Floyd, 1977), rocks from the NIP can be classified as subalkaline dacites and rhyolites (Fig. 7a, b).

The rare earth element (REE) concentrations of the NIP rocks are fairly homogeneous, displaying a high content of light REEs

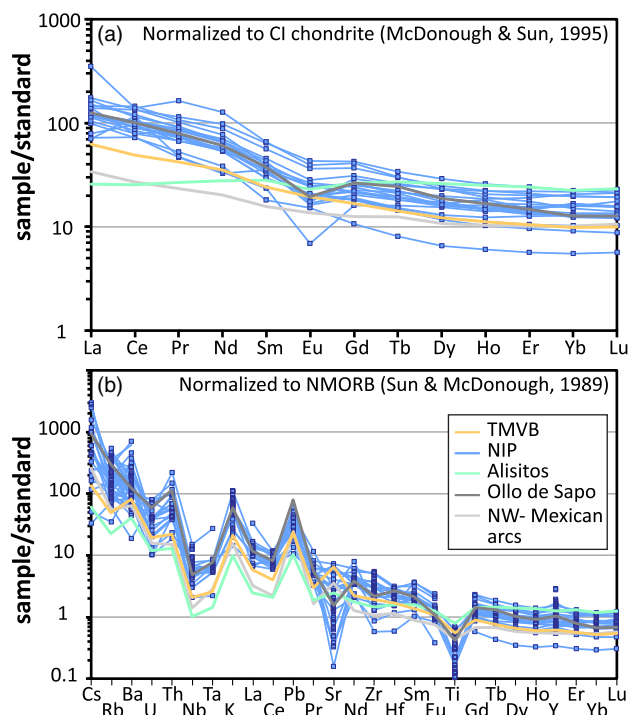


Fig. 8. (Colour online) (a) Chondrite-normalized rare earth element patterns of the NIP rocks. (b) normal - mid ocean ridge basalt (N-MORB) normalized trace-element patterns of the NIP rocks. Added for comparison are the average compositions of the Mexican arcs and the Ollo de Sapo magmatic suite. Values are normalized to CI chondrite (McDonough & Sun, 1995) and N-MORB (Sun & McDonough, 1989).

(LREE; average $La_N = 133.02$; ‘N’ values are normalized to CI chondrite from McDonough & Sun, 1995) and flat heavy REE (HREE) patterns, with moderate LREE/HREE ratios (average $La_N/Yb_N = 8.76$; Fig. 8a). Compared to modern and ancient Mexican oceanic and continental arc rocks, samples from the NIP display an overall higher REE fractionation (TMVB average $La_N/Yb_N = 6.29$; Alisitos–Guerrero arc average $La_N/Yb_N = 1.15$; NW Mexican arc average $La_N/Yb_N = 3.35$). Multi-element patterns resemble those of arc rocks (Fig. 8b); however, relative to modern and ancient arcs in Mexico, rocks of the NIP show a higher content of most trace elements, either large ion lithophile elements (LILEs), high field strength elements (HFSEs) or LREEs (Fig. 8b). Most of the NIP rocks also display low Sr concentrations and Sr/Nb ratios, together with negative Eu anomalies (Figs 8, 11).

The isotopic compositions of the whole rocks and zircon grains from the NIP suggest the contribution of an isotopically enriched source. In the Sr–Nd systems, for instance, the NIP rocks from central Mexico (Real de Catorce and Villa Juárez; Barboza-Gudiño *et al.* 2021) display $^{87}Sr/^{86}Sr$ and $^{143}Nd/^{144}Nd$ initial compositions that are more enriched compared to modern and ancient Mexican oceanic and continental arc rocks, even relative to the most enriched compositions of the active continental arc (i.e. the TMVB), and exhibit average continental values (Fig. 9a). The initial $\epsilon Hf(t)$ compositions of detrital zircons from Lower–Middle Jurassic sedimentary deposits (Ortega-Flores *et al.* 2020), from the Cretaceous Alisitos–Guerrero island arc (Contreras-López *et al.* 2018; Montaña-Cortes *et al.* 2019) and from modern sediments of western Mexico (Cavazos-Tovar *et al.* 2020) show that Early–Middle Jurassic zircons related to the NIP display mostly negative $\epsilon Hf(t)$ values (from -13 to $+5$), in contrast to the positive values ($+2$ to $+14$) that characterize

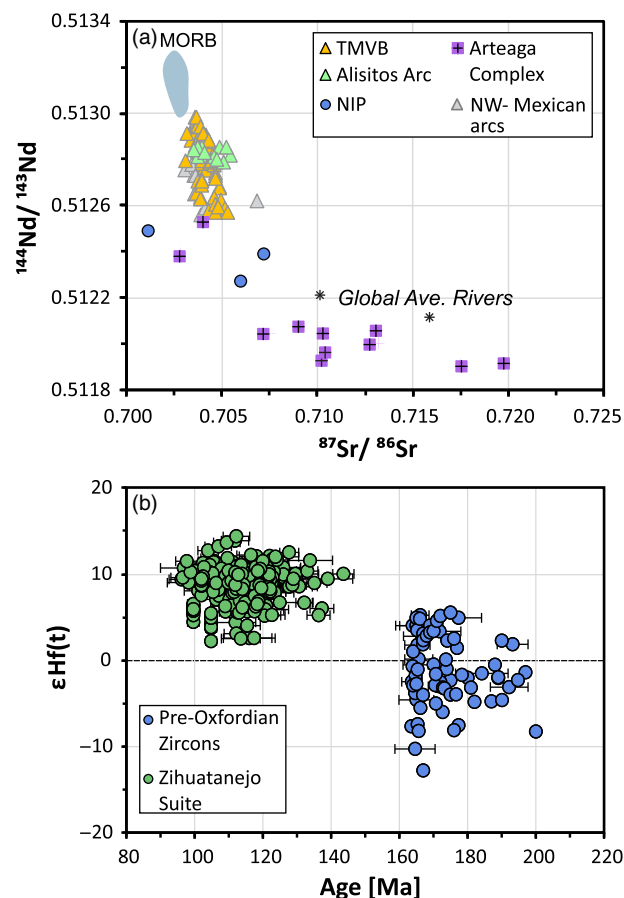


Fig. 9. (Colour online) (a) Initial bulk rock $^{143}Nd/^{144}Nd$ versus $^{87}Sr/^{86}Sr$ of dated NIP rocks (Barboza-Gudiño *et al.* 2021; we excluded sample VAR 07-16c, which displays an anomalously low $^{87}Sr/^{86}Sr$ initial ratio, indicative of a later thermal reset), the Alisitos and TMVB arc rocks (Morris *et al.* 2019; Parolari *et al.* 2021), and metamorphic lithologies from the Arteaga Complex (Centeno-García *et al.* 1993; Potra *et al.* 2014; Schaaf *et al.* 2020). Arteaga Complex data initial ratios have been recalculated to $t = 220$ Ma. The averages of river water suspended material (Goldstein & Jacobsen, 1988) are also displayed as a proxy of continental compositions. (b) Initial Hf isotopic compositions versus age of detrital zircons associated with the NIP (pre-Oxfordian zircons are a selection of crystals older than 163.5 Ma from the Cuale-Macias suite in Cavazos-Tovar *et al.* 2020; Ortega-Flores *et al.* 2020), and the Zihuatanejo arc (Zihuatanejo suite in Contreras-López *et al.* 2018; Montaña-Cortes *et al.* 2019; Cavazos-Tovar *et al.* 2020). Horizontal error bars represent available 2σ uncertainties of individual U–Pb ages.

zircons of Cretaceous age, associated with the construction of island arcs (e.g. Centeno-García, 2017; Fig. 9b). These low $\epsilon Hf(t)$ values displayed by zircon grains of Jurassic age (i.e. the ‘Cuale-Macias Suite’ in Cavazos-Tovar *et al.* 2020), coupled with their marked Eu anomalies, have been associated with the involvement of significant volumes of crustal melts derived from the fusion of fertile continental sedimentary rocks (Cavazos-Tovar *et al.* 2020).

5. A critical view of the arc-signature concept: use and misuse

Rocks from the NIP show high concentrations of fluid-mobile elements (e.g. LILEs) and depletions in HFSEs, a feature that has been widely interpreted as an arc signature, specifically the subduction influence on arc magmatism (e.g. Miller *et al.* 1994; Stolper & Newman, 1994). However, these geochemical attributes

are not exclusive to arc products but are found in many kind of rocks, such as most clastic continental and oceanic deposits (Goldschmidt, 1933; Shaw *et al.* 1967; Rudnick & Gao, 2003; Plank, 2013) that are commonly derived from arcs, but are evidently not arc rocks and do not necessarily relate directly to a contemporaneous arc setting. Since the continental crust as a whole shows this geochemical signature (e.g. Taylor *et al.* 1983; Rudnick & Gao, 2003), it is likely that any rocks derived either from erosion or melting of crustal rocks (e.g. S-type granites), as well as most magma that interacts with the continental crust during its ascent, would adopt its compositions, even if they were formed in a tectonic setting away from the influence of any subduction zone. On the other hand, not all the magmatic rocks that compose modern and ancient arcs exhibit this subduction influence. For instance, many magmas from the TMVB do not show an arc signature, but rather an intraplate-like affinity, although these were undoubtedly emplaced in a continental arc setting (Gómez-Tuena *et al.* 2018*b* and references therein).

Critically, the assignment of an arc signature is only appropriate when applied to true mantle melts, i.e. magmas that originated from melting of a mantle lithology. Interestingly, a subduction influence has recently been reported in a significant number of mid-ocean ridge basalts (MORB), suggesting that it could be a pervasive feature in some portions of the upper mantle itself, without the need for being associated with an active subduction zone (Yang *et al.* 2021). Moreover, the chemical signal of subduction may also be carried to the deep mantle as evidenced by the isotopic compositions of some intraplate basalts (Hart, 1988; Stracke *et al.* 2005).

Hence, the arc-like features shown by the NIP are definitively not a strong argument for classifying its tectonic environment as a magmatic arc. More generally, we believe that the concept of arc signature must be handled judiciously, especially when dealing with ancient rocks that do not represent true mantle melts. When the tectonic setting is contested and there are not magmatic rocks that represent true mantle melts, as appears to be the case for the NIP, the discussion of the petrogenesis of a magmatic suite should go beyond the recognition of an arc signature, since it may not represent a discriminant, but rather a compositional attribute of many geological materials. For instance, the examination of the style and extent of trace-element fractionation, the employment of petrological models, the measurement of initial isotopic values of whole rocks and related zircons, as well as the comparison with other well-known magmatic suites can help discern the tectonic setting.

6. Petrogenesis of the NIP

The main goal of this study is to discuss whether the NIP magmatic event was related to the development of a Jurassic arc or whether it represents the igneous manifestation of a continental rift associated with the long-term regional extension triggered by Pangaea's break-up. We compared the chemical features of the NIP with other well-studied magmatic suites (data sources are in the caption of Fig. 7), represented by two emblematic Mexican magmatic arcs, the Alisito–Guerrero island arc and the TMVB continental arc, together with the Jurassic to Cretaceous arc complexes in Central and Southern Baja California and the felsic rocks from the Ollo de Sapo magmatic suite. The latter are located in northern Spain and are thought to represent almost pure upper-crustal sediment melts generated by tectonic extension in an intracontinental or back-arc rift setting related to the Palaeozoic opening of the

Rheic ocean (Montes *et al.* 2010; Villaseca *et al.* 2014; Díaz-Alvarado *et al.* 2016). Moreover, since felsic rocks like those of the NIP may represent derivative liquids of a parental mafic melt, we also performed fractional crystallization models on both major and trace elements to address whether this assumption is feasible and to constrain the eventual chemical features of this putative mafic source. Finally, to test whether the felsic nature of the NIP magmas represents a primary feature, and not the secondary product of mafic melts, we also discuss the composition of NIP rocks in light of the results from experimental studies on sediment melting.

The pervasive occurrence of felsic and strongly peraluminous magmas, coupled with the lack of intermediate and mafic products, represents an outstanding feature of the NIP. Though these kinds of melts are not abundant on Earth, they have been reported in many orogenic (e.g. Harris *et al.* 1986; Harris & Massey, 1994; Nabelek, 2020) and extensional settings, both arc and non-arc related (e.g. Kanaris-Sotiriou *et al.* 1993; Bryan *et al.* 2000; García-Arias *et al.* 2018). Conversely, volcanic arcs mainly comprise mafic and intermediate, metaluminous, calc-alkaline rocks (e.g. Gill, 1981). While felsic magmas are indeed present in arc settings, they are volumetrically subordinate to basalts and andesites, with peraluminous rhyolites being an uncommon feature of subduction-related magmatism (Turner & Langmuir, 2015). Simple Rhyolite-MELTS (Gualda *et al.* 2012) modelling results indicate that the major-element concentrations of the NIP rocks are inconsistent with protracted fractional crystallization of a putative parental arc magma (Fig. 7c, d; more details in the figure caption), and likewise that felsic rocks from the NIP do not gain their peraluminosity through a process of crystal fractionation. Rhyolite-MELTS also provides the bulk composition and the amount of crystallized phases at each crystallization step. Therefore, using a compilation of suitable partition coefficients (K_ds; online Supplementary Material Table S2), consistent with the changes in major-element composition of the liquid at each step, it was possible to calculate the trace-element concentrations of the crystallizing magma. The results (red lines of Fig. 10) clearly show that the high concentrations of many trace elements exhibited by the NIP magmas are not predicted by crystal fractionation models of a mafic arc melt, even at high silica contents and fractionation level (SiO₂ ~75 % and X ~74 %; model constraints in the caption of Fig. 10). Still, the concentrations of several incompatible elements, which are expected to increase steadily during crystal fractionation, are scattered and poorly related to the SiO₂ concentration (Fig. 10). This evidence, together with the peraluminous trend of the NIP magmas (Fig. 7e), suggests that fractionation of a parental arc magma is unlikely to have generated compositions like those of the NIP.

Compared to intraplate and MOR basalts, arc magmas are notably enriched in Sr and depleted in Nb, as a result of the subduction influence (e.g. Stolper & Newman, 1994). As rocks from the TMVB and Alisito–Guerrero arc show an overall high Sr concentration at variable Nb values (Fig. 10e), and given that concentrations of these same elements in the NIP magmas are not the result of fractional crystallization of a parental arc liquid, the Sr/Nb ratio can potentially be used to separate arc magmatic sources from non-arc ones. In addition, considering that Rb and Nb are highly incompatible elements, the Rb/Nb ratio is expected to be almost invariant during processes of crystal fractionation (Fig. 10f) and should reflect the primitive ratio of the magmatic source. Remarkably, in Figure 11, magmas of the NIP and the Mexican arcs form two distinct clusters, implying unrelated magmatic sources.

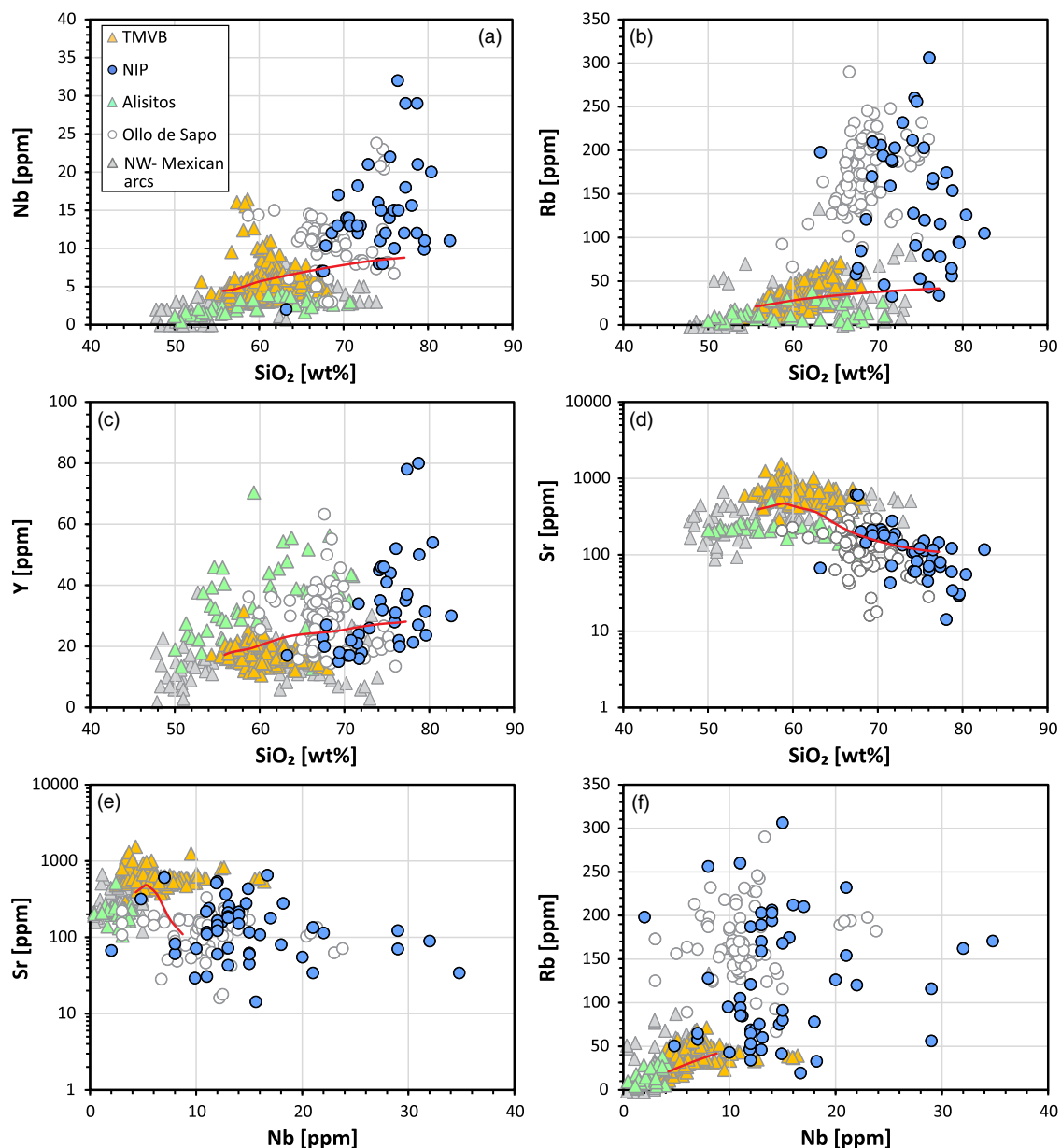


Fig. 10. (Colour online) Concentrations of some incompatible trace elements of the NIP rocks. Compared to arc products, NIP rocks show scattered and generally higher values, similar to the Ollo de Sapo magmatic suite. Red lines represent fractional crystallization paths calculated from the results of the Rhyolite-MELTS experiment described in the caption of Figure 7. Fractional crystallization models for trace elements are calculated considering the variable proportions of crystallizing minerals at different liquid compositions, accordingly to the results of the Rhyolite-MELTS experiment. Individual mineral partition coefficient (K_d) values and sources are reported in online Supplementary Material Table S2.

On one hand, the low Sr/Nb ratios displayed by the NIP rocks reinforce the notion of a non-arc genesis. On the other, since intraplate basalts are characterized by very low Rb/Nb ratios (<1; Sun & McDonough, 1989) and because of the overall invariance of this ratio during fractional crystallization, the data also discard an origin from fractionation of a parental intraplate basalt. Interestingly, the felsic magmas of the Ollo de Sapo suite overlap the NIP compositional cluster, strongly suggesting a similar magmatic origin.

Experimental studies demonstrate that peraluminosity and high SiO₂ contents are common features in pure sediment melts (SiO₂ ≥70%; Patiño Douce, 2000), over a wide range of pressure–temperature (P – T) and protolith compositions under fluid-absent condition (e.g. Montel & Vielzeuf, 1997). Since these

features are ubiquitous in nearly all Early–Middle Jurassic magmas of southern and central Mexico, we now investigate the involvement of a sedimentary source in the genesis of the NIP.

Peraluminous crustal melts are believed to originate through dehydration-melting reactions under fluid-absent or fluid-deficient conditions (e.g. Thompson, 1982; Clemens *et al.* 2020). Muscovite, biotite and hornblende are the most common hydrous minerals that undergo those reactions (e.g. Patiño Douce, 2000). The incongruent breakdown of these minerals, in fact, provides alkali and water to the newly forming melt, while MgO, FeO, Al₂O₃ and CaO are preferentially stored in more refractory peritectic mineral species (Patiño Douce, 2000). In this way, crustal melts are characterized by low contents of these latter elements, while, in contrast, high concentrations of these same elements

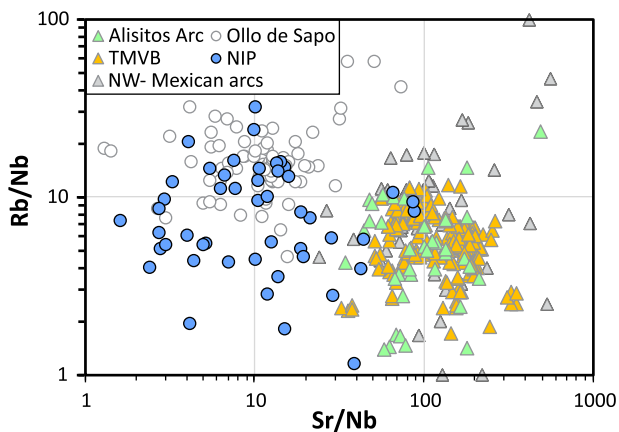


Fig. 11. (Colour online) Rb/Nb versus Sr/Nb variation diagram showing compositional differences between NIP rocks and Mexican arc rocks, suggesting a different magmatic evolution from a separate source.

are a common attribute of most mantle-derived melts, regardless of the tectonic setting (e.g. Gill, 1981; Baker *et al.* 1995). The major-element contents of the NIP rocks entirely overlap the compositions of experimental melts of a metasedimentary source (Fig. 7).

The low CaO contents of the NIP magmas suggest that their potential residual assemblage was composed of plagioclase and/or Ca-garnet in different proportions (Montel & Vielzeuf, 1997; Patiño Douce, 2000). However, since the HREEs are rarely fractionated, and most of the NIP magmas show a strong Eu negative anomaly coupled with low Sr/Nb ratios (Figs 8a, 11), it is likely that the unmolten solid contained abundant plagioclase as the main Ca-rich phase. Residual plagioclase has been widely observed in low-pressure experimental melts of sandstones and pelites (Montel & Vielzeuf, 1997; Patiño Douce, 2000; Clemens *et al.* 2020). At higher pressure (>1 GPa), or in the presence of aqueous fluids accompanying melting, plagioclase becomes unstable, with Ca being mainly incorporated into grossular and diopside (Patiño Douce & Beard, 1996; Patiño Douce, 2000; Brown, 2013). Moreover, the high K_2O/Na_2O ratio of the NIP magmas (average 6.25) suggests that the main source of these melts is likely a felsic sedimentary or metasedimentary rock, as melting of mafic rocks (i.e. basalts and amphibolites) produces trondhjemitic melts that are strongly depleted in K relative to melts derived from mica-rich sources (Rapp *et al.* 1991; Rapp & Watson, 1995; Patiño Douce, 2000). The high K_2O/Na_2O ratios of the NIP magmas also suggests fluid-absent conditions during partial melting, since H_2O fluxing of (meta)sedimentary rocks would produce melts that are noticeably enriched in Na_2O/K_2O (Collins *et al.* 2020), a feature that is further enhanced when melting occurs at high P (Patiño Douce & Beard, 1996; Patiño Douce & Harris, 1998). The geochemical evidence thus suggests shallow melting (<0.8–1.0 GPa) of a felsic (meta)sedimentary source in the absence of free fluids.

The enriched isotopic composition of the NIP rocks supports the involvement of a sedimentary or metasedimentary protolith in the genesis of this magmatic province (Fig. 9a). According to the geological record, Upper Triassic submarine fan deposits (Zacatecas and La Ballena formations, Arteaga and El Chilar complexes; Centeno-García, 2005; Ortega-Flores *et al.* 2014) accreted to the western equatorial margin of Pangaea are the most suitable candidate to represent the source of the NIP rocks. These metasedimentary rocks are mainly metapelite and metasandstone showing enriched isotopic compositions

(Centeno-García *et al.* 1993) that are similar to those of the NIP (Fig. 9a). Likewise, the overall negative $\epsilon Hf(t)$ shown by the magmatic zircons related to the NIP supports this hypothesis, indicating the involvement of an enriched source (Fig. 9b). Also, many rocks from the NIP display a significant amount of inherited zircon grains (Godínez-Urban *et al.* 2011; Zavala-Monsiváis *et al.* 2012; R. F. Durán-Aguilar, unpub. Master's thesis, Univ. Nacional Autónoma de México, 2013; Silva-Romo *et al.* 2015; Barboza-Gudiño *et al.* 2021) with ages that span between Triassic and Proterozoic times (Fig. 12a). They show age groups that are virtually identical to the ones of the Upper Triassic metasedimentary rocks (Fig. 12b), implying that these lithologies are a viable (meta)sedimentary source for the NIP.

The geochemical and isotopic evidence presented above suggests that the NIP is likely the result of fluid-absent melting of these Triassic metasedimentary rocks. However, melts produced experimentally from dehydration melting of micaceous metamorphic rocks yield SiO_2 contents ≥ 70 wt % (Patiño Douce, 2000). Since at least some samples from the NIP have lower values (Fig. 7a, b), it is likely that a mafic mantle-related component is also involved in the genesis of these magmas. This is also suggested by the positive ϵNd initial values displayed by some NIP rocks (Barboza-Gudiño *et al.* 2021) and the positive $\epsilon Hf(t)$ values in a few Early–Middle Jurassic zircons from modern sediments (Cavazos-Tovar *et al.* 2020). Although mafic and ultramafic rocks are not present in our set of NIP rocks, we speculate on the nature of this mafic component.

For instance, the average zircon saturation temperature ($T_{zircSat}$; Watson & Harrison, 1983) calculated for Early–Middle Jurassic zircons found in modern sediments (Cavazos-Tovar *et al.* 2020), here used as a proxy for zircons crystallized from the NIP magmas, indicates that the magmatic temperature was below 824 ± 44 °C (1σ) to preserve inherited zircon grains from being completely resorbed. At the same time, the predicted temperature for the crystallization of NIP magmatic zircon is 735 ± 52 °C (1σ). This has been calculated using the Ti-in-zircon thermometer (T_{zircTi} ; $\text{Log}(T_{in\ zircon}) = (6.01 \pm 0.03) - ((503 \pm 30)/T(K))$; Watson *et al.* 2006; details about the Ti measurements of zircons are reported in Cavazos-Tovar *et al.* 2020) on pre-Oxfordian zircons (Fig. 9b). The results allow the inference of the temperature of formation of the NIP magmas to be at least 735 °C, but not markedly higher than 825 °C, and definitely below the ~ 1030 °C, which is the liquidus temperature calculated for an average composition of the NIP magmas using the Rhyolite-MELTS software (Gualda *et al.* 2012). If we consider a (meta)pelitic source for the NIP magmas, then pressure must not exceed ~ 0.8 GPa to maintain a garnet-free residue in this temperature interval (e.g. Brown, 2013), in agreement with the overall low La_N/Yb_N exhibited by the NIP rocks (Fig. 8a). At these conditions, melting is predicted to start with the breakdown of muscovite to form K-feldspar, at ~ 700 – 750 °C, followed by the progressive dissolution of quartz and feldspar, with biotite as the main ferromagnesian residual phase below ~ 850 – 900 °C (e.g. Brown, 2013). At higher temperatures, melting continues with the breakdown of biotite, leaving a refractory residue composed of orthopyroxene and cordierite. However, considering the average $T_{zircSat}$ temperature of 824 ± 44 °C (1σ) estimated for the NIP magmas, we believe that a temperature of magma generation below 900 – 850 °C is in line with the widespread occurrence of inherited zircons in these rocks. The amount of melt predicted by experimental modelling should be ~ 10 – 30 % at these P – T conditions (Montel & Vielzeuf, 1997), which is above the physical threshold

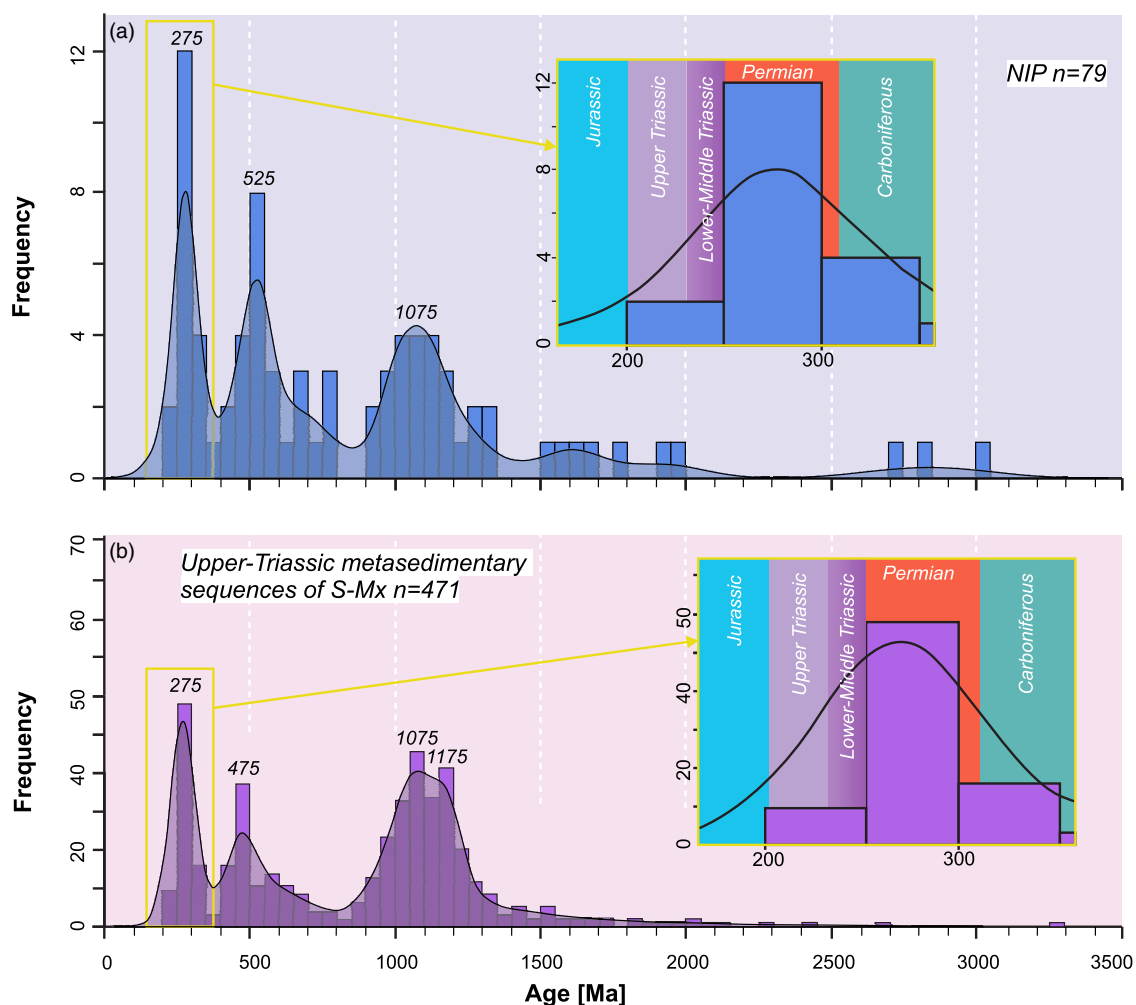


Fig. 12. (Colour online) (a) Kernel density distribution (KDE; Vermeesch, 2018) of inherited zircons found in magmatic rocks from the NIP (Godínez-Urban *et al.* 2011; Zavala Monsiváis *et al.* 2012; R. F. Durán-Aguilar, unpub. Master's thesis, Univ. Nacional Autónoma de México, 2013; Silva-Romo *et al.* 2015; Barboza-Gudiño *et al.* 2021) and (b) detrital zircons from the Upper Triassic metasedimentary rock sequences of southern Mexico (Martini *et al.* 2009; Ortega-Flores *et al.* 2016; Ortega-Flores *et al.* 2020). Yellow boxes are a magnification of the zircon frequency distribution centred on the Permian (275 Ma).

to reach the melt connectivity transition allowing the melt to migrate (Rosenberg & Handy, 2005). Such P – T conditions cannot be attained in a crust characterized by a normal geothermal gradient of 25 – 30 °C km^{-1} ; therefore, an additional source of heat is needed in order to melt sediments at such a shallow depth (≤ 25 km). Accordingly, we considered that the underplating of basalts could be a viable mechanism to provide the necessary amount of heat to melt the (meta)sedimentary source of the NIP. Because of the geochemical features of the NIP magmas, and the fact that continental primitive arc magmas (i.e. orogenic andesites) might be not sufficiently hot to trigger crustal melting (~ 100 to 250 °C less compared to ocean-island-basalt-like basalts; Díaz-Bravo *et al.* 2014; Zellmer *et al.* 2016; Gómez-Tuena *et al.* 2018a), we tentatively suggest that the heat source was represented by the injection of intraplate basalts in an attenuated continental crust. The absence of such basalts in the NIP, however, is problematic. A possible explanation for the lack of these mafic rocks could be the modest volume of basalt production during the NIP event, compared to the spatial extent of Upper Triassic metasedimentary sequences in southern and central Mexico, which potentially represented very fertile (e.g. fusible) rocks. In such a scenario, it would be very difficult for a basalt to reach the surface without

assimilating some amount of metasedimentary host rocks. Alternatively, the felsic NIP magmas could have formed a rheological barrier, trapping the mafic rocks at depth (e.g. Murphy, 2020). In any case, the majority of these mafic magmas would have likely crystallized at depth as a consequence of heat exchange with the metasedimentary layer that produced the NIP felsic melts. Even in the case that some of the NIP parental magmas reached the surface, they would likely have experienced some degree of crustal contamination and achieved intermediate compositions. A small production of mantle melting is also supported by the relatively small volumes of NIP rocks that are currently preserved in the stratigraphic record of southern and central Mexico.

7. Tectonic model

Our new interpretation of the NIP challenges previously published Early–Middle Jurassic tectonic scenarios for southern Mexico. Most models for Early and Middle Jurassic time imply that subduction was continuous along the Pacific margin of North and South America (Fig. 4). The chemical composition of the NIP rocks, however, questions the interpretation of this province as a continental magmatic arc. Instead, data here presented suggest that

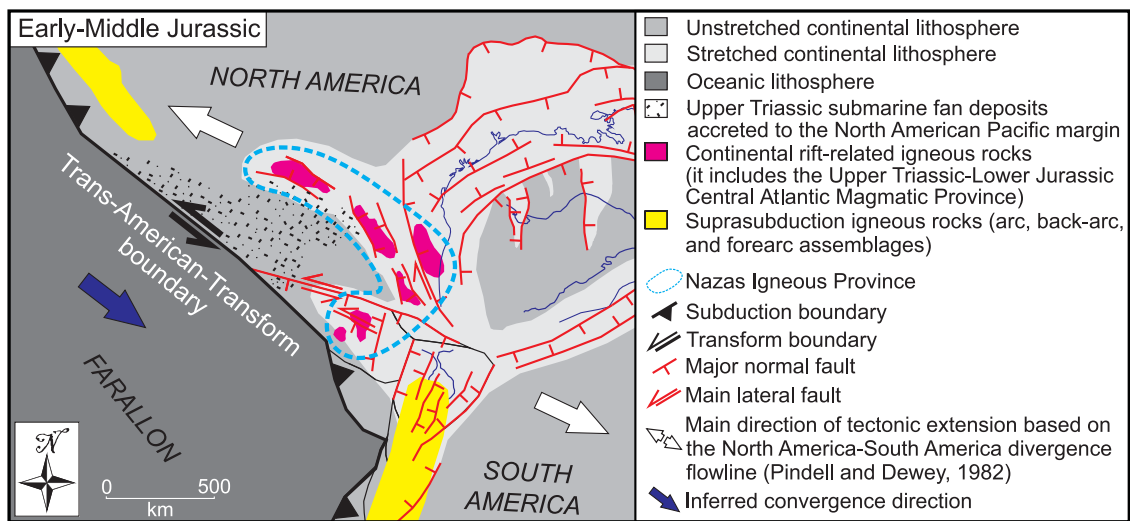


Fig. 13. (Colour online) Geotectonic reconstruction of the North America – South America divergent boundary during Early–Middle Jurassic time (~190–170 Ma; after Boschman *et al.* 2014; Bayona *et al.* 2020; Erlich & Pindell, 2021 and Pindell *et al.* 2021). The reconstruction shows the novel interpretation of the Nazas province as a magmatic province related to the continental rift between North and South America. In this new scenario, we propose that the Mexican segment of the North American margin was a transform boundary.

the NIP is likely related to sediment melting in a tectonic setting that is not necessarily associated with subduction. These sediment melts could have formed during a regional-scale extensional event that affected wide portions of the present-day southern United States, Mexico and northwestern South America (Fig. 13) and that is well documented in central and southern Mexico by the development of several Early and Middle Jurassic extensional to transtensional sedimentary basins (Goldhammer, 1999; Martini & Ortega-Gutiérrez, 2018). This regional-scale extension began in Middle Triassic time in the proto-GM and continued in central and southern Mexico culminating with the GM opening (e.g. Erlich & Pindell, 2021; Pindell *et al.* 2021). In this context, the NIP may represent a syn-rift igneous province associated with the continental attenuation that preceded the opening of the GM, which is not necessarily related to the Pacific tectonic evolution of North America, but rather a consequence of Pangaea fragmentation.

Indeed, the complex and non-linear spatial distribution of the volcanic centres of the NIP is difficult to interpret as a back-arc suite either, as it should exhibit an alignment (sub-)parallel to the palaeo-trench, and because no coeval arc rocks of the same age have been reported in central and southern Mexico. Moreover, the mere existence of the Upper Triassic metasedimentary successions negates the back-arc setting hypothesis for the NIP. In effect, Upper Triassic successions were accreted to the Pacific margin of Mexico before the end of Triassic time and constituted the western continental edge of southernmost North America by the beginning of Jurassic time. If a hypothetical Early–Middle Jurassic arc existed, then it must have been subducted along the adjacent trench, together with the currently exposed Upper Triassic successions that would have formed part of the fore-arc region.

Based on our reinterpretation of the NIP, we propose the existence of a Triassic–Middle Jurassic transform fault, here named the Trans-America-transform boundary, that connected the North and South American subduction zones (Fig. 13). Evidence of sinistral block motion along the Mexican continental margin during at least Early and Middle Jurassic time is provided by the occurrence

of kilometre-scale, WNW-trending, brittle to brittle-ductile left-lateral faults, which controlled the architecture and evolution of major transtensional basins in southern Mexico (Martiny *et al.* 2012; Zepeda-Martínez *et al.* 2021). Therefore, these major left-lateral faults may be interpreted as the inboard expression of the Trans-America-transform boundary along the Mexican continental margin. Although this structure has not been directly documented, the geological evidence of such a boundary may have been erased by a complex history punctuated by distinct tectonic events such as subduction erosion and terrane accretion (Morán-Zenteno *et al.* 1996; Scholl & von Huene, 2007; Keppie *et al.* 2012; Martini *et al.* 2012, 2013; Centeno-García, 2017; Parolari *et al.* 2018; Cavazos-Tovar *et al.* 2020).

8. Tectonic implications

The reinterpretation of the NIP as a result of rift-related magmatism offers a new perspective on the Jurassic tectonic evolution of central and southern Mexico. The first and most obvious implication is that subduction initiation beneath the southern and central segments of the Mexican continental margin must be younger than Middle Jurassic time. As a consequence, during Early–Middle Jurassic time, most of the Mexican sector of North America may not represent a convergent margin but instead could be envisioned as a passive or conservative one. Yet, the hypothesis of a conservative margin appears to be more likely for several reasons. An Early–Middle Jurassic Mexican passive margin would have implied the existence of two transform faults that connected this part of the margin with the subduction zones directly northward and southward. However, there is no geological evidence that such lithospheric structures were active during Early and Middle Jurassic time in Mexico. Moreover, numerical models indicate that passive margins are too stable for subduction initiation (Nikolaeva *et al.* 2011; Stern & Gerya, 2018) and, besides, there is no documented example of a passive margin collapsing into a subduction zone in Mesozoic and Cenozoic times (Stern & Gerya, 2018; Arculus *et al.* 2019). Conversely, during Cenozoic time many

subduction zones of the western Pacific developed on former transform boundaries as a response to changes in plate motions (Arculus *et al.* 2019 and references therein). Numerical models also support this hypothesis, predicting that conservative margins represent the most favourable sites where new subduction zones are expected to arise (Stern & Gerya, 2018 and references therein). In the case of Mexico, the scenario that we propose for Early–Middle Jurassic time would meet the two fundamental requirements for subduction initiation (Stern & Gerya, 2018): (1) the presence of a long (>100 km) lithospheric weakness, i.e. the Trans-America-transform proposed in this work (Fig. 13) and (2) the existence of a density contrast between the oceanic Farallon plate and the North America continent.

The predicted time for the onset of subduction in southern and central Mexico roughly coincides with the beginning of the GM opening (~167–163 Ma; Cantú-Chapa, 2009; Pindell *et al.* 2021). In our view, this event may represent a cause–effect relationship. Specifically, the production of new oceanic crust in the GM may have produced enough tectonic force to initiate subduction in Mexico, converting the proposed Late Triassic–Middle Jurassic conservative margin into a subduction zone by the end of Middle Jurassic or the beginning of Late Jurassic times. The early manifestation of arc magmatism in Baja California (~165–160 Ma; Kimbrough & Moore, 2003; Contreras-López *et al.* 2021) also supports the onset of subduction by the end of Middle Jurassic time along the central and southern sectors of the Mexican margin, consistent with the proposed time lapse between the subduction initiation and the onset of arc magmatism (~7 Ma; Arculus *et al.* 2019). In this view, we suggest that the onset of subduction in southern and central Mexico during late Middle Jurassic time was triggered by changes in plate motions related to the opening of the GM, as a result of the Atlantic-related extensional tectonic regime associated with Pangaea break-up.

To conclude, in the same way that the present-day architecture of the North American margin is composed of a complex mosaic of subduction zones connected together by transform faults (Fig. 1), mainly as a result of the Farallon–Pacific oceanic ridges subduction (Plafker & Berg, 1994; Atwater & Stock, 1998; Aragón *et al.* 2020), we consider that, during Jurassic time, the western American margin was probably composed of both convergent and conservative sectors. Though we cannot prove that subduction of one or more oceanic ridges was going on during Early–Middle Jurassic time, deep seismic tomographic images of the mantle below the Atlantic Ocean shows a number of anomalous low-velocity zones that have been interpreted as the remnants of ancient subducted Farallon-related slabs (van der Meer *et al.* 2018). This suggests that, during Mesozoic time, subduction was not truly continuous along the western margin of North America, and that the subduction of more than one oceanic plate represents a feasible scenario.

Supplementary material. To view supplementary material for this article, please visit <https://doi.org/10.1017/S0016756822000061>

Acknowledgements. This work is part of M. Parolari postdoctoral research supported by ‘Programa de Becas Posdoctorales de la UNAM (Universidad Nacional Autónoma de México)’, Mexico. Productive discussions with Laura Mori were helpful in the development of this research. The manuscript benefited greatly from the thoughtful reviews of Brendan Murphy, Nancy Riggs, Iain Neill and two anonymous reviewers.

Declaration of interest. The authors declare that they have no known competing financial interests or personal relationships that could have appeared to influence the work reported in this paper.

References

- Anderson TH, McKee JW and Jones NW (1990) Jurassic (?) melange in north-central Mexico. *Geological Society of America Abstracts with Programs* **22**, 3.
- Aragón E, D’Eramo F, Cuffaro M, Doglioni C, Ficini E, Pinotti L, Nacif S, Demartis M, Hernando I and Fuentes T (2020) The westward lithospheric drift, its role on the subduction and transform zones surrounding Americas: Andean to cordilleran orogenic types cyclicity. *Geoscience Frontiers* **11**, 1219–29.
- Arculus RJ, Gurnis M, Ishizuka O, Reagan MK, Pearce JA and Sutherland R (2019) How to create new subduction zones: a global perspective. *Oceanography* **32**, 160–74.
- Atwater T and Stock J (1998) Pacific-north America plate tectonics of the Neogene southwestern united states: an update. *International Geology Review* **40**, 375–402.
- Baker MB, Hirschmann MM, Ghiorso MS and Stolper EM (1995) Compositions of near-solidus peridotite melts from experiments and thermodynamic calculations. *Nature* **375**, 308–11.
- Barboza-Gudiño JR, Hoppe M, Gómez-Anguiano M and Martínez-Macias PR (2004) Contributions to the stratigraphic and structural interpretation of the northwestern portion of the Sierra de Catorce, San Luis Potosí, Mexico. *Revista Mexicana de Ciencias Geológicas* **21**, 299–319.
- Barboza-Gudiño JR, Orozco-Esquivel MT, Gómez-Anguiano M and Zavala-Monsiváis A (2008) The Early Mesozoic volcanic arc of western North America in northeastern Mexico. *Journal of South American Earth Sciences* **25**, 49–63.
- Barboza-Gudiño JR, Zavala-Monsiváis A, Castellanos-Rodríguez V, Jaime-Rodríguez D and Almaraz-Martínez C (2021) Subduction-related Jurassic volcanism in the Mesa Central province and contemporary Gulf of Mexico opening. *Journal of South American Earth Sciences* **108**, 102961. doi: 10.1016/j.jsames.2020.102961.
- Barboza-Gudiño JR, Zavala-Monsiváis A, Venegas-Rodríguez G and Barajas-Nigoche LD (2010) Late Triassic stratigraphy and facies from northeastern Mexico: tectonic setting and provenance. *Geosphere* **6**, 621–40.
- Bartolini C, Lang H and Spell T (2003) Geochronology, geochemistry, and tectonic setting of the Mesozoic Nazas arc in north-central Mexico, and its continuation to northern South America. In *The Circum-Gulf of Mexico and the Caribbean: Hydrocarbon Habitats, Basin Formation and Plate Tectonics* (eds C Bartolini, RT Buffler and JF Blickwede), pp. 79–82. American Association of Petroleum Geologists Memoir no. 79.
- Bas MJL, Maitre RWL, Streckeisen A and Zanettin B (1986) A chemical classification of volcanic rocks based on the total alkali-silica diagram. *Journal of Petrology* **27**, 745–50.
- Bayona G, Bustamante C, Nova G and Salazar-Franco AM (2020) Jurassic evolution of the northwestern corner of Gondwana: present knowledge and future challenges in studying Colombian Jurassic rocks. In *The Geology of Colombia, vol. 2 Mesozoic* (eds J Gómez and AO Pinilla-Pachon), pp. 171–207. Bogotá: Servicio Geológico Colombiano, Publicaciones Geológicas Especiales 36.
- Bayona G, Jiménez G, Silva C, Cardona A, Montes C, Roncancio J and Cordani U (2010) Paleomagnetic data and K–Ar ages from Mesozoic units of the Santa Marta massif: a preliminary interpretation for block rotation and translations. *Journal of South American Earth Sciences* **29**, 817–31.
- Bird D and Burke K (2006) Pangea breakup: Mexico, Gulf of Mexico, and Central Atlantic Ocean. *SEG Technical Program Expanded Abstracts 2006*, 1013–17a.
- Boschman LM, van Hinsbergen DJJ, Torsvik TH, Spakman W and Pindell JL (2014) Kinematic reconstruction of the Caribbean region since the early Jurassic. *Earth-Science Reviews* **138**, 102–36.

- Brown M** (2013) Granite: from genesis to emplacement. *Geological Society of America Bulletin* **125**, 1079–113.
- Bryan SE, Ewart A, Stephens CJ, Parianos J and Downes PJ** (2000) The Whitsunday Volcanic Province, Central Queensland, Australia: lithological and stratigraphic investigations of a silicic-dominated large igneous province. *Journal of Volcanology and Geothermal Research* **99**, 55–78.
- Busby-Spera CJ** (1988) Speculative tectonic model for the early Mesozoic arc of the southwest Cordilleran United States. *Geology* **16**, 1121–5.
- Busby-Spera CJ, Martinson JM, Riggs NR and Schermer ER** (1990) The Triassic–Jurassic magmatic arc in the Mojave-Sonoran deserts and the Sierran-Klamath region; similarities and differences in paleogeographic evolution. In *Paleozoic and Early Mesozoic Paleogeographic Relations; Sierra Nevada, Klamath Mountains, and Related Terranes* (eds DS Harwood and MM Miller), pp. 325–37. Geological Society of America, Special Papers vol. 255.
- Campa-Uranga MF, García Díaz JL and Iriondo A** (2004) El arco sedimentario del Jurásico Medio (Grupo Tecocoyunca y Las Lluvias) de Olinálá. *GEOS: Unión Geofísica Mexicana* **24**, 174.
- Cantú-Chapa A** (2009) Upper Jurassic stratigraphy (Oxfordian and Kimmeridgian) in petroleum wells of Campeche Shelf, Gulf of Mexico. In *Petroleum Systems in the Southern Gulf of Mexico*. (eds C Bartolini and JR Román Ramos), pp. 79–91. American Association of Petroleum Geologists Memoir no. 90.
- Cavazos-Tovar JG, Gómez-Tuena A and Parolari M** (2020) The origin and evolution of the Mexican Cordillera as registered in modern detrital zircons. *Gondwana Research* **86**, 83–103.
- Centeno-García E** (2005) Review of Upper Palaeozoic and Lower Mesozoic stratigraphy and depositional environments of central and west Mexico: constraints on terrane analysis and paleogeography. In *The Mojave-Sonora Megashield Hypothesis: Development, Assessment, and Alternatives* (eds TH Anderson, JA Nourse, JW McKee and MB Steiner), pp. 233–58. Geological Society of America, Special Papers vol. 393.
- Centeno-García E** (2017) Mesozoic tectono-magmatic evolution of Mexico: an overview. *Ore Geology Reviews* **81**, 1035–52.
- Centeno-García E, Ruis J, Coney PJ, Patchett PJ and Ortega-Gutiérrez F** (1993) Guerrero terrane of Mexico: its role in the southern Cordillera from new geochemical data. *Geology* **21**, 419–22.
- Centeno-García E and Silva-Romo G** (1997) Petrogenesis and tectonic evolution of Central Mexico during Triassic–Jurassic time. *Revista Mexicana de Ciencias Geológicas* **14**, 244–60.
- Clemens JD, Stevens G and Bryan SE** (2020) Conditions during the formation of granitic magmas by crustal melting: hot or cold; drenched, damp or dry? *Earth-Science Reviews* **200**, 102982. doi: [10.1016/j.earscirev.2019.102982](https://doi.org/10.1016/j.earscirev.2019.102982).
- Collins WJ, Murphy JB, Johnson TE and Huang HQ** (2020) Critical role of water in the formation of continental crust. *Nature Geoscience* **13**, 331–8.
- Contreras-López M, Delgado-Argote LA, Weber B, Torres-Carrillo XG, Frei D and Gómez-Alvarez DK** (2021) Petrogenesis of the meta-igneous rocks of the Sierra El Arco and coeval magmatic rocks in Baja California: Middle Jurassic–Early Cretaceous (166–140 Ma) island arc magmatism of NW México. *International Geology Review* **63**, 1153–80.
- Contreras-López M, Delgado-Argote LA, Weber B and Valencia V** (2018) Petrology and geochronology of the Calmallí pluton: insights to the suture zone between island arc and continental crusts in the southern Peninsular Ranges batholith, Baja California, México. *Journal of South American Earth Sciences* **88**, 568–88.
- Coombs HE, Kerr AC, Pindell J, Buchs D, Weber B and Solari L** (2020) Petrogenesis of the crystalline basement along the western Gulf of Mexico: postcollisional magmatism during the formation of Pangea. In *Southern and Central Mexico: Basement Framework, Tectonic Evolution, and Provenance of Mesozoic–Cenozoic Basins* (eds U Martens and RS Molina Garza). Geological Society of America, Special Papers, published online 23 August 2020. doi: [10.1130/2020.2546\(02\)](https://doi.org/10.1130/2020.2546(02)).
- Correa-Martínez AM, Rodríguez G, Arango MI, Zapata G and Bermúdez JG** (2016) *Catálogo de Unidades Litoestratigráficas de Colombia: Batolito de Mogotes, Cordillera Oriental, Departamento de Santander*. Medellín: Servicio Geológico Colombiano, 112 pp.
- Díaz-Alvarado J, Fernández C, Chichorro M, Castro A and Pereira MF** (2016) Tracing the Cambro-Ordovician ferrosilicic to calc-alkaline magmatic association in Iberia by in situ U–Pb SHRIMP zircon geochronology (Gredos massif, Spanish Central System batholith). *Tectonophysics* **681**, 95–110.
- Díaz-Bravo BA, Gómez-Tuena A, Ortega-Obregón C and Pérez-Arvizu O** (2014) The origin of intraplate magmatism in the western Trans-Mexican volcanic belt. *Geosphere* **10**, 340–73.
- Dickinson WR** (2009) Anatomy and global context of the North American Cordillera. In *Backbone of the Americas: Shallow Subduction, Plateau Uplift, and Ridge and Terrane Collision* (eds S Mahlburg Kay, VA Ramos and WR Dickinson), pp. 1–29. Geological Society of America, Memoirs no. 204.
- Dickinson WR and Lawton TF** (2001) Carboniferous to Cretaceous assembly and fragmentation of Mexico. *Geological Society of America Bulletin* **113**, 1142–60.
- Elías Herrera M and Sánchez Zavala J** (1990) Tectonic implications of a mylonitic granite in the lower structural levels of the Tierra Caliente complex (Guerrero terrane), southern Mexico. *Revista Mexicana de Ciencias Geológicas* **9**, 113–25.
- Elías-Herrera M, Sánchez-Zavala JL and Macías-Romo C** (2000) Geologic and geochronologic data from the Guerrero terrane in the Tejuipilco area, southern Mexico: new constraints on its tectonic interpretation. *Journal of South American Earth Sciences* **13**, 355–75.
- Erlich RN and Pindell J** (2021) Crustal origin of the West Florida Terrane, and detrital zircon provenance and development of accommodation during initial rifting of the southeastern Gulf of Mexico and western Bahamas. In *The Basins, Orogens and Evolution of the Southern Gulf of Mexico and Northern Caribbean* (eds I Davison, JNF Hull and J Pindell), 77–118. Geological Society of London, Special Publication no. 504.
- Fastovsky DE, Hermes OD, Strater NH, Bowring SA, Clark JM, Montellano M and Hernandez RR** (2005) Pre-Late Jurassic, fossil-bearing volcanic and sedimentary red beds of Huizachal Canyon, Tamaulipas, Mexico. *The Mojave-Sonora Megashield Hypothesis: Development, Assessment, and Alternatives* (eds TH Anderson, JA Nourse, JW McKee and MB Steiner), pp. 401–26. Geological Society of America, Special Papers vol. 393.
- Frederick BC, Blum MD, Snedden JW and Fillon RH** (2020) Early Mesozoic synrift Eagle Mills Formation and coeval siliciclastic sources, sinks, and sediment routing, northern Gulf of Mexico basin. *Geological Society of America Bulletin* **132**, 2631–50.
- García-Arias M, Díez-Montes A, Villaseca C and Blanco-Quintero IF** (2018) The Cambro-Ordovician Ollo de Sapo magmatism in the Iberian Massif and its Variscan evolution: a review. *Earth-Science Reviews* **176**, 345–72.
- Gill JB** (1981) Bulk chemical composition of orogenic andesites. In *Orogenic Andesites and Plate Tectonics*, pp. 97–167. Minerals and Rocks. Berlin: Springer-Verlag.
- Godínez-Urban A, Lawton TF, Molina Garza RS, Iriondo A, Weber B and López-Martínez M** (2011) Jurassic volcanic and sedimentary rocks of the La Silla and Todos Santos Formations, Chiapas: record of Nazas arc magmatism and rift-basin formation prior to opening of the Gulf of Mexico. *Geosphere* **7**, 121–44.
- Goldhammer RK** (1999) Mesozoic sequence stratigraphy and paleogeographic evolution of northeast Mexico. In *Mesozoic Sedimentary and Tectonic History of North-Central Mexico* (eds C Bartolini, JL Wilson and TF Lawton), pp. 1–58. Geological Society of America, Special Papers vol. 340.
- Goldschmidt VM** (1933) Grundlagen der quantitativen Geochemie. *Fortschritte der Mineralogie, Kristallographie und Petrographie* **17**, 112–56.
- Goldstein SJ and Jacobsen SB** (1988) Nd and Sr isotopic systematics of river water suspended material: implications for crustal evolution. *Earth and Planetary Science Letters* **87**, 249–65.
- Gómez-Tuena A, Cavazos-Tovar JG, Parolari M, Straub SM and Espinasa-Pereña R** (2018a) Geochronological and geochemical evidence of continental crust ‘relamination’ in the origin of intermediate arc magmas. *Lithos* **322**, 52–66.
- Gómez-Tuena A, Mori L and Straub SM** (2018b) Geochemical and petrological insights into the tectonic origin of the Transmexican Volcanic Belt. *Earth-Science Reviews* **183**, 153–81.
- González-León CM, Vázquez-Salazar M, Navarro TS, Solari LA, Nourse JA, del Rio-Salas R, Lozano-Santacruz R, Arvizu OP and**

- Valenzuela Chacón JC** (2021) Geology and geochronology of the Jurassic magmatic arc in the Magdalena quadrangle, north-central Sonora, Mexico. *Journal of South American Earth Sciences* **108**, 103055. doi: [10.1016/j.jsames.2020.103055](https://doi.org/10.1016/j.jsames.2020.103055).
- Gualda GAR, Ghorso MS, Lemons RV and Carley TL** (2012) Rhyolite-MELTS: a modified calibration of MELTS optimized for silica-rich, fluid-bearing magmatic systems. *Journal of Petrology* **53**, 875–90.
- Harris N and Massey J** (1994) Decompression and anatexis of Himalayan metapelites. *Tectonics* **13**, 1537–46.
- Harris NBW, Pearce JA and Tindle AG** (1986) Geochemical characteristics of collision-zone magmatism. In *Collision Tectonics* (eds NBW Harris, JA Pearce and AG Tindle), pp. 67–81. Geological Society of London, Special Publication no. 19.
- Hart SR** (1988) Heterogeneous mantle domains: signatures, genesis and mixing chronologies. *Earth and Planetary Science Letters* **90**, 273–96.
- Haxel GB, Wright JE, Riggs NR, Tosdal RM and May DJ** (2005) Middle Jurassic Topawa group, Baboquivari Mountains, south-central Arizona: volcanic and sedimentary record of deep basins within the Jurassic magmatic arc. In *The Mojave-Sonora Megashield Hypothesis: Development, Assessment, and Alternatives* (eds TH Anderson, JA Nourse, JW McKee and MB Steiner), pp. 329–57. Geological Society of America, Special Papers vol. 393.
- Heatherington AL and Mueller PA** (1991) Geochemical evidence for Triassic rifting in southwestern Florida. *Tectonophysics* **188**, 291–302.
- Heatherington AL and Mueller PA** (1999) Lithospheric sources of North Florida, USA tholeiites and implications for the origin of the Suwannee terrane. *Lithos* **46**, 215–33.
- Heatherington AL and Mueller PA** (2003) Mesozoic igneous activity in the Suwannee terrane, Southeastern USA: petrogenesis and Gondwanan affinities. *Gondwana Research* **6**, 296–311.
- Heffner DM, Knapp JH, Akintunde OM and Knapp CC** (2012) Preserved extent of Jurassic flood basalt in the South Georgia Rift: a new interpretation of the J horizon. *Geology* **40**, 167–70.
- Helbig M, Keppie JD, Murphy JB and Solari LA** (2012) U–Pb geochronological constraints on the Triassic–Jurassic Ayú Complex, southern Mexico: derivation from the western margin of Pangea-A. *Gondwana Research* **22**, 910–27.
- Heron PJ** (2019) Mantle plumes and mantle dynamics in the Wilson cycle. In *Fifty Years of the Wilson Cycle Concept in Plate Tectonics* (eds RW Wilson, GA Houseman, KJW McCaffrey, AG Doré and SJH Buitter), pp. 87–103. Geological Society of London, Special Publication no. 470.
- Hill RI** (1991) Starting plumes and continental break-up. *Earth and Planetary Science Letters* **104**, 398–416.
- Hole MJ** (2015) The generation of continental flood basalts by decompression melting of internally heated mantle. *Geology* **43**, 311–14.
- Irvine TN and Baragar WRA** (1971) A guide to the chemical classification of the common volcanic rocks. *Canadian Journal of Earth Sciences* **8**, 523–48.
- Jones NW, McKee JW, Anderson TH and Silver LT** (1995) Jurassic volcanic rocks in northeastern Mexico: a possible remnant of a Cordilleran magmatic arc. In *Studies on the Mesozoic of Sonora and Adjacent Areas* (eds C Jacques-Ayala, CM González-Léon and J Roldán-Quintana), pp. 179–90. Geological Society of America, Special Papers vol. 301.
- Kanaris-Sotiriou R, Morton AC and Taylor PN** (1993) Palaeogene peraluminous magmatism, crustal melting and continental breakup: the Erlend Complex, Faeroe-Shetland Basin, NE Atlantic. *Journal of the Geological Society, London* **150**, 903–14.
- Kay RW and Kay SM** (1988) Crustal recycling and the Aleutian arc. *Geochimica et Cosmochimica Acta* **52**, 1351–9.
- Keppie DE, Hynes AJ, Lee JKWW and Norman M** (2012) Oligocene–Miocene back-thrusting in southern Mexico linked to the rapid subduction erosion of a large forearc block. *Tectonics* **31**, 1–17.
- Keppie JD, Nance RD, Dostal J, Ortega-Rivera A, Miller BV, Fox D, Muise J, Powell JT, Mumma SA and Lee JWK** (2004) Mid-Jurassic tectonothermal event superposed on a Palaeozoic geological record in the Acatlán Complex of southern Mexico: hotspot activity during the breakup of Pangea. *Gondwana Research* **7**, 238–60.
- Kimbrough DL and Moore TE** (2003) Ophiolite and volcanic arc assemblages on the Vizcaino Peninsula and Cedros Island, Baja California Sur, México: Mesozoic forearc lithosphere of the Cordilleran magmatic arc. In *Tectonic Evolution of Northwestern Mexico and the Southwestern USA* (eds SE Johnson, SR Paterson, JM Fletcher, GH Girty, DL Kimbrough and A Martín-Barajas), pp. 43–71. Geological Society of America, Special Papers vol. 374.
- Kinoshita O** (2002) Possible manifestations of slab window magmatism in Cretaceous southwest Japan. *Tectonophysics* **344**, 1–13.
- Kirsch M, Helbig M, Keppie JD, Murphy JB, Lee JKW and Solari LA** (2014) A Late Triassic tectonothermal event in the eastern Acatlán Complex, southern Mexico, synchronous with a magmatic arc hiatus: the result of flat-slab subduction? *Lithosphere* **6**, 63–79.
- Klitgord KD, Hutchinson DR and Schouten H** (1988) U.S. Atlantic continental margin; structural and tectonic framework. In *The Atlantic Continental Margin* (ed. RE Sheridan and JA Grow), pp. 19–55. Boulder, CO: Geological Society of America.
- Labails C, Olivet JL, Aslanian D and Roest WR** (2010) An alternative early opening scenario for the Central Atlantic Ocean. *Earth and Planetary Science Letters* **297**, 355–68.
- Lawton TF and Molina Garza RS** (2014) U–Pb geochronology of the type Nazas Formation and superjacent strata, northeastern Durango, Mexico: implications of a Jurassic age for continental-arc magmatism in north-central Mexico. *Geological Society of America Bulletin* **126**, 1181–99.
- Lawton TF, Uruña JER, Solari LA, Terrazas CT, Juárez-Arriaga E and Ortega-Obrigón C** (2018) Provenance of Upper Triassic–Middle Jurassic strata of the Plomos uplift, east-central Chihuahua, Mexico, and possible sedimentologic connections with Colorado Plateau depositional systems. In *Tectonics, Sedimentary Basins, and Provenance: A Celebration of the Career of William R. Dickinson* (eds RV Ingersoll, TF Lawton and SA Graham), pp. 481–507. Geological Society of America, Special Papers vol. 540.
- Le Roy P and Piqué A** (2001) Triassic–Liassic western Moroccan synrift basins in relation to the Central Atlantic opening. *Marine Geology* **172**, 359–81.
- López Infanzón M** (1986) Estudio petrogenético de las Rocas Igneas en las Formaciones Huizachal y Nazas. *Boletín de la Sociedad Geológica Mexicana* **47**, 1–41.
- López-Isaza JA and Zuluaga CA** (2020) Late Triassic to Jurassic magmatism in Colombia: implications for the evolution of the northern margin of South America. In *The Geology of Colombia, vol. 2 Mesozoic* (eds J Gómez and AO Pinilla-Pachon), pp. 77–116. Bogotá: Servicio Geológico Colombiano, Publicaciones Geológicas Especiales 36.
- Martini M, Ferrari L, López-Martínez M, Cerca-Martínez M, Valencia VA and Serrano-Duran L** (2009) Cretaceous–Eocene magmatism and Laramide deformation in southwestern Mexico: no role for terrane accretion. In *Backbone of the Americas: Shallow Subduction, Plateau Uplift, and Ridge and Terrane Collision* (eds S Mahlburg Kay, VA Ramos and WR Dickinson), pp. 151–82. Geological Society of America, Memoirs no. 204.
- Martini M, Fitz E, Solari L, Camprubí A, Hudleston PJ, Lawton TF, Tolson G and Centeno-García E** (2012) The Late Cretaceous fold-thrust belt in the Peña de Bernal–Tamazunchale area and its possible relationship to the accretion of the Guerrero Terrane. In *GSA Field Guide 25: The Southern Cordillera and Beyond* (eds JJ Aranda-Gómez, G Tolson and RS Molina-Garza), pp. 19–38. Boulder, CO: Geological Society of America.
- Martini M and Ortega-Gutiérrez F** (2018) Tectono-stratigraphic evolution of eastern Mexico during the break-up of Pangea: a review. *Earth-Science Reviews* **183**, 38–55.
- Martini M, Solari L and Camprubí A** (2013) Kinematics of the Guerrero terrane accretion in the Sierra de Guanajuato, central Mexico: new insights for the structural evolution of arc-continent collisional zones. *International Geology Review* **55**, 574–89.
- Martin-Rojas I, Somma R, Delgado F, Estévez A, Iannace A, Perrone V and Zamparelli V** (2009) Triassic continental rifting of Pangea: direct evidence from the Alpujarride carbonates, Betic Cordillera, SE Spain. *Journal of the Geological Society, London* **166**, 447–58.
- Martiny BM, Morán-Zenteno DJ, Tolson G, Silva-Romo G and López-Martínez M** (2012) The Salado River fault: reactivation of an early Jurassic fault in a transfer zone during Laramide deformation in southern Mexico. *International Geology Review* **54**, 144–64.

- Marzen RE, Shillington DJ, Lizarralde D, Knapp JH, Heffner DM, Davis JK and Harder SH (2020) Limited and localized magmatism in the Central Atlantic Magmatic Province. *Nature Communications* **11**, 1–8.
- Marzoli A, Callegaro S, dal Corso J, Davies JHFL, Chiaradia M, Youbi N, Bertrand H, Reisberg L, Merle R and Jourdan F (2018) The Central Atlantic Magmatic Province (CAMP): a review. In *The Late Triassic World* (ed. LH Tanner), pp. 91–125. Topics in Geobiology, vol. 46. Cham: Springer.
- Maus S, Barckhausen U, Berkenbosch H, Bournas N, Brozina J, Childers V, Dostaler F, Fairhead JD, Finn C, von Frese RRB, Gaina C, Golynsky S, Kucks R, Lühr H, Milligan P, Mogren S, Müller RD, Olesen O, Pilkington M, Saltus R, Schreckenberger B, Thébaud E and Tontini FC (2009) EMAG2: a 2-arc min resolution Earth Magnetic Anomaly Grid compiled from satellite, airborne, and marine magnetic measurements. *Geochemistry, Geophysics, Geosystems* **10**, Q08005. doi: [10.1029/2009GC002471](https://doi.org/10.1029/2009GC002471).
- McDonough WF and Sun SS (1995) The composition of the Earth. *Chemical Geology* **120**, 223–53.
- Mickus K, Stern RJ, Keller GR and Anthony EY (2009) Potential field evidence for a volcanic rifted margin along the Texas Gulf Coast. *Geology* **37**, 387–90.
- Miller DM, Goldstein SL and Langmuir CH (1994) Cerium/lead and lead isotope ratios in arc magmas and the enrichment of lead in the continents. *Nature* **368**, 514–20.
- Molina-Garza RS, Lawton TF, Figueroa-Guadarrama A and Pindell J (2020) Mexican record of circum-Gulf of Mexico Jurassic depositional systems and climate. In *Southern and Central Mexico: Basement Framework, Tectonic Evolution, and Provenance of Mesozoic–Cenozoic Basins* (eds U Martens and RS Molina-Garza). Geological Society of America, Special Papers, published online 23 August 2020. doi: [10.1130/2020.2546\(13\)](https://doi.org/10.1130/2020.2546(13)).
- Montaño-Cortes PC, Molina-Garza RS and Iriondo A (2019) Paleomagnetismo e isotopos de Hf en rocas del cretácico inferior del terreno guerrero, bahía chamela e isla cocinas (Jalisco, Mexico): implicaciones tectónicas. *Revista Mexicana de Ciencias Geológicas* **36**, 289–307.
- Montel JM and Vielzeuf D (1997) Partial melting of metagreywackes, Part II. compositions of minerals and melts. *Contributions to Mineralogy and Petrology* **128**, 176–96.
- Montes AD, Catalán JRM and Mulas FB (2010) Role of the Ollo de Sapo massive felsic volcanism of NW Iberia in the Early Ordovician dynamics of northern Gondwana. *Gondwana Research* **17**, 363–76.
- Morán-Zenteno DJ, Corona-Chavez P and Tolson G (1996) Uplift and subduction erosion in southwestern Mexico since the Oligocene: pluton geobarometry constraints. *Earth and Planetary Science Letters* **141**, 51–65.
- Morgan WJ (1983) Hotspot tracks and the early rifting of the Atlantic. *Tectonophysics* **94**, 123–39.
- Morris RA, Debari SM, Busby C, Medynski S and Jicha BR (2019) Building arc crust: plutonic to volcanic connections in an extensional oceanic arc, the Southern Alisitos Arc, Baja California. *Journal of Petrology* **60**, 1195–228.
- Müller RD, Zahirovic S, Williams SE, Cannon J, Seton M, Bower DJ, Tetley MG, Heine C, le Breton E, Liu S, Russell SHJ, Yang T, Leonard J and Gurnis M (2019) A global plate model including lithospheric deformation along major rifts and orogens since the Triassic. *Tectonics* **38**, 1884–907.
- Murphy JB (2020) Appinite suites and their genetic relationship with coeval voluminous granitoid batholiths. *International Geology Review* **62**, 683–713.
- Nabelek PI (2020) Petrogenesis of leucogranites in collisional orogens. In *Post-Archean Granitic Rocks: Petrogenetic Processes and Tectonic Environments* (eds V Janoušek, B Bonin, WJ Collins, F Farina and P Bowden), pp. 179–207. Geological Society of London, Special Publication no. 491.
- Nesbitt HW and Young GM (1982) Early Proterozoic climates and plate motions inferred from major element chemistry of lutites. *Nature* **299**, 715–7.
- Nikolaeva K, Gerya TV and Marques FO (2011) Numerical analysis of subduction initiation risk along the Atlantic American passive margins. *Geology* **39**, 463–6.
- O'Hara D, Karlstrom L and Ramsey DW (2020) Time-evolving surface and subsurface signatures of Quaternary volcanism in the Cascades arc. *Geology* **48**, 1088–93.
- Ohta T and Arai H (2007) Statistical empirical index of chemical weathering in igneous rocks: a new tool for evaluating the degree of weathering. *Chemical Geology* **240**, 280–97.
- Ortega-Flores B, Solari LA and de Jesús Escalona-Alcázar F (2016) The Mesozoic successions of western Sierra de Zacatecas, central Mexico: provenance and tectonic implications. *Geological Magazine* **153**, 696–717.
- Ortega-Flores B, Solari L, Lawton TF and Ortega-Obregón C (2014) Detrital-zircon record of major Middle Triassic–Early Cretaceous provenance shift, central Mexico: demise of Gondwanan continental fluvial systems and onset of back-arc volcanism and sedimentation. *International Geology Review* **56**, 237–61.
- Ortega-Flores B, Solari LA and Martini M (2021) Multidimensional Scaling (MDS): a quantitative approximation of zircon ages to sedimentary provenance with some examples from Mexico. *Journal of South American Earth Sciences* **110**, 103347. doi: [10.1016/j.jsames.2021.103347](https://doi.org/10.1016/j.jsames.2021.103347).
- Ortega-Flores B, Solari LA, Martini M and Ortega-Obregón C (2020) The Guerrero terrane, a para-autochthonous block on the paleo-Pacific continental margin of North America: evidence from zircon U–Pb dating and Hf isotopes. In *Southern and Central Mexico: Basement Framework, Tectonic Evolution, and Provenance of Mesozoic–Cenozoic Basins* (eds U Martens and RS Molina-Garza). Geological Society of America, Special Papers, published online 23 August 2020. doi: [10.1130/2020.2546\(08\)](https://doi.org/10.1130/2020.2546(08)).
- Parolari M, Gómez-Tuena A, Cavazos-Tovar JG and Hernández-Quevedo G (2018) A balancing act of crust creation and destruction along the western Mexican convergent margin. *Geology* **46**, 455–8.
- Parolari M, Gómez-Tuena A, Errázuriz-Henao C and Cavazos-Tovar JG (2021) Orogenic andesites and their link to the continental rock cycle. *Lithos* **382–383**, 105958. doi: [10.1016/j.lithos.2020.105958](https://doi.org/10.1016/j.lithos.2020.105958).
- Patiño Douce AE (2000) What do experiments tell us about the relative contributions of crust and mantle to the origin of granitic magmas? In *Understanding Granites: Integrating New and Classical Techniques* (eds A Castro, C Fernández and JL Vigneresse), pp. 55–75. Geological Society of London, Special Publication no. 168.
- Patiño Douce AE and Beard JS (1996) Effects of P, f(O₂) and Mg/Fe ratio on dehydration melting of model metagreywackes. *Journal of Petrology* **37**, 999–1024.
- Patiño Douce AE and Harris N (1998) Experimental constraints on Himalayan anatexis. *Journal of Petrology* **39**, 689–710.
- Pérez-Gutiérrez R, Solari LA, Gómez-Tuena A and Martens U (2009) Mesozoic geologic evolution of the Xolapa migmatitic complex north of Acapulco, southern Mexico: implications for paleogeographic reconstructions. *Revista Mexicana de Ciencias Geológicas* **26**, 201–21.
- Perri F (2020) Chemical weathering of crystalline rocks in contrasting climatic conditions using geochemical proxies: an overview. *Palaeogeography, Palaeoclimatology, Palaeoecology* **556**, 109873. doi: [10.1016/j.palaeo.2020.109873](https://doi.org/10.1016/j.palaeo.2020.109873).
- Pilger RH (1981) Plate reconstructions, aseismic ridges, and low-angle subduction beneath the Andes. *Geological Society of America Bulletin* **92**, 448–56.
- Pindell J and Dewey JF (1982) Permo-Triassic reconstruction of western Pangea and the evolution of the Gulf of Mexico/Caribbean region. *Tectonics* **1**, 179–211.
- Pindell JL and Kennan L (2009) Tectonic evolution of the Gulf of Mexico, Caribbean and northern South America in the mantle reference frame: an update. In *The Origin and Evolution of the Caribbean Plate* (eds KH James, MA Lorente and JL Pindell), pp. 1–55. Geological Society of London, Special Publication no. 328.
- Pindell J, Villagómez D, Molina-Garza R, Graham R and Weber B (2021) A revised synthesis of the rift and drift history of the Gulf of Mexico and surrounding regions in the light of improved age dating of the Middle Jurassic salt. In *The Basins, Orogens and Evolution of the Southern Gulf of Mexico and Northern Caribbean* (eds I Davison, JNF Hull and J Pindell), pp. 29–76. Geological Society of London, Special Publication no. 504.
- Pindell J, Weber B, Hale-Erlich W, Cossey S, Bitter M, Molina Garza R, Graham R and Erlich RN (2020) Strontium isotope dating of evaporites and the breakup of the Gulf of Mexico and Proto-Caribbean Seaway.

- In *Southern and Central Mexico: Basement Framework, Tectonic Evolution, and Provenance of Mesozoic–Cenozoic Basins* (eds U Martens and RS Molina-Garza). Geological Society of America, Special Papers, published online 23 August 2020. doi: [10.1130/2020.2546\(12\)](https://doi.org/10.1130/2020.2546(12)).
- Plafker G and Berg HC** (eds) (1994) *The Geology of Alaska*. Boulder, CO: Geological Society of America.
- Plank T** (2013) The chemical composition of subducting sediments. In *Treatise on Geochemistry, 2nd Edition* (eds HD Holland and KK Turekian), pp. 607–29. Oxford: Elsevier Ltd.
- Pompa-Mera V, Schaaf P, Hernández-Treviño T, Weber B, Solís-Pichardo G, Villanueva-Lascrain D and Layer P** (2013) Geology, geochronology, and geochemistry of Isla María Madre, Nayarit, Mexico. *Revista Mexicana de Ciencias Geológicas* **30**, 1–23.
- Potra A, Hickey-Vargas R, Macfarlane AW and Salters VJM** (2014) Pb, Sr, and Nd isotopic characteristics of a variety of lithologies from the Guerrero composite terrane, west-central Mexico: constraints on their origin. *Revista Mexicana de Ciencias Geológicas* **31**, 203–20.
- Quandt D, Trumbull RB, Altenberger U, Cardona A, Romer RL, Bayona G, Duca M, Valencia V, Vásquez M, Cortes E and Guzman G** (2018) The geochemistry and geochronology of Early Jurassic igneous rocks from the Sierra Nevada de Santa Marta, NW Colombia, and tectono-magmatic implications. *Journal of South American Earth Sciences* **86**, 216–30.
- Rapp RP and Watson EB** (1995) Dehydration melting of metabasalt at 8–32 kbar: implications for continental growth and crust–mantle recycling. *Journal of Petrology* **36**, 891–931.
- Rapp RP, Watson EB and Miller CF** (1991) Partial melting of amphibolite/eclogite and the origin of Archean trondhjemites and tonalites. *Precambrian Research* **51**, 1–25.
- Riel N, Jaillard E, Martelat JE, Guillot S and Braun J** (2018) Permian–Triassic Tethyan realm reorganization: implications for the outward Pangea margin. *Journal of South American Earth Sciences* **81**, 78–86.
- Riggs NR, Oberling ZA, Howell ER, Parker WG, Barth AP, Cecil MR and Martz JW** (2016) Sources of volcanic detritus in the basal Chinle Formation, southwestern Laurentia, and implications for the Early Mesozoic magmatic arc. *Geosphere* **12**, 439–63.
- Riggs NR, Reynolds SJ, Lindner PJ, Howell ER, Barth AP, Parker WG and Walker JD** (2013) The early Mesozoic Cordilleran arc and late Triassic paleogeography: the detrital record in upper Triassic sedimentary successions on and off the Colorado Plateau. *Geosphere* **9**, 602–13.
- Rosenberg CL and Handy MR** (2005) Experimental deformation of partially melted granite revisited: implications for the continental crust. *Journal of Metamorphic Geology* **23**, 19–28.
- Rubio-Cisneros II and Lawton TF** (2011) Detrital zircon U–Pb ages of sandstones in continental red beds at Valle de Huizachal, Tamaulipas, NE Mexico: record of Early–Middle Jurassic arc volcanism and transition to crustal extension. *Geosphere* **7**, 159–70.
- Rudnick RL and Gao S** (2003) Composition of the continental crust. *Treatise on Geochemistry* **3–9**, 1–64.
- Sahabi M, Aslanian D and Olivet JL** (2004) Un nouveau point de départ pour l'histoire de l'Atlantique central. *Comptes Rendus Geoscience* **336**, 1041–52.
- Schaaf P, Díaz-López F, Gutiérrez-Aguilar F, Solís-Pichardo G, Hernández-Treviño T, Arrieta-García G, Solari L and Ortega-Obregón C** (2020) Geochronology and geochemistry of the Puerto Vallarta igneous and metamorphic complex and its relation to Cordilleran arc magmatism in northwestern Mexico. *Lithos* **352–353**, 105248. doi: [10.1016/j.lithos.2019.105248](https://doi.org/10.1016/j.lithos.2019.105248).
- Schettino A and Turco E** (2009) Breakup of Pangaea and plate kinematics of the central Atlantic and Atlas regions. *Geophysical Journal International* **178**, 1078–97.
- Schliche RW** (2003) 4. Progress in understanding the structural geology, basin evolution, and tectonic history of the eastern North American Rift System. In *The Great Rift Valleys of Pangea in Eastern North America* (eds P LeTourneau and P Olsen), pp. 21–64. New York: Columbia University Press.
- Scholl DW and von Huene R** (2007) Crustal recycling at modern subduction zones applied to the past – issues of growth and preservation of continental basement crust, mantle geochemistry, and supercontinent reconstruction. In *4-D Framework of Continental Crust* (eds RD Hatcher, MP Carlson, JH McBride and JR Martínez Catalán), pp. 9–32. Geological Society of America, Memoirs no. 200.
- Schoonmaker A and Kidd WSF** (2006) Evidence for a ridge subduction event in the Ordovician rocks of north-central Maine. *Geological Society of America Bulletin* **118**, 897–912.
- Shaw DM, Reilly GA, Muysson JR, Pattenden GE and Campbell FE** (1967) An estimate of the chemical composition of the Canadian Precambrian shield. *Canadian Journal of Earth Sciences* **4**, 829–53.
- Silva-Romo G, Arellano-Gil J, Mendoza-Rosales C and Nieto-Obregón J** (2000) A submarine fan in the Mesa Central, Mexico. *Journal of South American Earth Sciences* **13**, 429–42.
- Silva-Romo G, Mendoza-Rosales CC, Campos-Madriral E, Centeno-García E and Peralta-Salazar R** (2015) Early Mesozoic Southern Mexico–Amazonian connection based on U–Pb ages from detrital zircons: the La Mora Paleo-River in the Mixteca Terrane and its paleogeographic and tectonic implications. *Gondwana Research* **28**, 689–701.
- Sisson VB, Pavlis TL, Roeske SM and Thorkelson DJ** (2003) Introduction: an overview of ridge–trench interactions in modern and ancient settings. In *Geology of a Transpressional Orogen Developed During Ridge–Trench Interaction Along the North Pacific Margin* (eds VB Sisson, SM Roeske and TL Pavlis), pp. 1–18. Geological Society of America, Special Papers vol. 371.
- Spencer CJ, Murphy JB, Hoiland CW, Johnston ST, Mitchell RN and Collins WJ** (2019) Evidence for whole mantle convection driving Cordilleran tectonics. *Geophysical Research Letters* **46**, 4239–48.
- Spikings R and Paul AN** (2019) The Permian – Triassic history of magmatic rocks of the northern Andes (Colombia and Ecuador): supercontinent assembly and disassembly. In *The Geology of Colombia, vol. 2 Mesozoic* (eds J Gómez and AO Pinilla-Pachon), pp. 1–43. Bogotá: Servicio Geológico Colombiano, Publicaciones Geológicas Especiales 36.
- Stern RJ and Gerya T** (2018) Subduction initiation in nature and models: a review. *Tectonophysics* **746**, 173–98.
- Stolper E and Newman S** (1994) The role of water in the petrogenesis of Mariana trough magmas. *Earth and Planetary Science Letters* **121**, 293–325.
- Stracke A, Hofmann AW and Hart SR** (2005) FOZO, HIMU, and the rest of the mantle zoo. *Geochemistry, Geophysics, Geosystems* **6**, Q05007. doi: [10.1029/2004GC000824](https://doi.org/10.1029/2004GC000824).
- Straub SM, Gómez-Tuena A, Stuart FM, Zellmer GF, Espinasa-Pereña R, Cai Y and Iizuka Y** (2011) Formation of hybrid arc andesites beneath thick continental crust. *Earth and Planetary Science Letters* **303**, 337–47.
- Sun SS and McDonough WF** (1989) Chemical and isotopic systematics of oceanic basalts: implications for mantle composition and processes. In *Magmatism in the Ocean Basins* (eds AD Saunders and MJ Norry), pp. 313–45. Geological Society of London, Special Publication no. 42.
- Talavera-Mendoza O** (2000) Mélanges in southern Mexico: geochemistry and metamorphism of Las Ollas complex (Guerrero terrane). *Canadian Journal of Earth Sciences* **37**, 1309–20.
- Taylor SR, McLennan SM and McCulloch MT** (1983) Geochemistry of loess, continental crustal composition and crustal model ages. *Geochimica et Cosmochimica Acta* **47**, 1897–905.
- Thompson AB** (1982) Dehydration melting of pelitic rocks and the generation of H₂O–undersaturated granitic liquids. *American Journal of Science* **282**, 1567–95.
- Torres-Carrillo XG, Delgado-Argote LA, Weber B and Contreras-López M** (2020) Early to Middle Jurassic San Andrés-Cedros plutonic suite, western coast of Baja California, Mexico: geochemical and isotopic evidence for an island arc extending to the central peninsula. *Journal of South American Earth Sciences* **98**, 102471. doi: [10.1016/j.jsames.2019.102471](https://doi.org/10.1016/j.jsames.2019.102471).
- Tosdal RM, Haxel GB and Wright JE** (1989) Jurassic geology of the Sonoran Desert region, southern Arizona, southeastern California, and northernmost Sonora; construction of a continental-margin magmatic arc. *Arizona Geological Society Digest* **17**, 397–434.
- Turner SJ and Langmuir CH** (2015) The global chemical systematics of arc front stratovolcanoes: evaluating the role of crustal processes. *Earth and Planetary Science Letters* **422**, 182–93.
- van der Lelij R, Spikings R, Ulianov A, Chiaradia M and Mora A** (2016) Palaeozoic to Early Jurassic history of the northwestern corner of

- Gondwana, and implications for the evolution of the Iapetus, Rheic and Pacific Oceans. *Gondwana Research* **31**, 271–94.
- van der Meer DG, van Hinsbergen DJJ and Spakman W** (2018) Atlas of the underworld: slab remnants in the mantle, their sinking history, and a new outlook on lower mantle viscosity. *Tectonophysics* **723**, 309–448.
- Vásquez-Serrano A, Nieto-Samaniego ÁF, Alaniz-Álvarez S and Rangel-Granados E** (2019) Shortening and kinematics of the Late Triassic rocks in the Tolimán area, central Mexico. *Journal of South American Earth Sciences* **95**, 102303. doi: [10.1016/j.jsames.2019.102303](https://doi.org/10.1016/j.jsames.2019.102303).
- Vega-Granillo R, Sarmiento-Villagrana A, Vidal-Solano JR, Araux-Sánchez E and Bourjac-de-Anda A** (2020) Northern limit of Gondwana in northwestern Mexico from detrital zircon data. *Gondwana Research* **83**, 232–47.
- Vermeesch P** (2018) IsoplotR: a free and open toolbox for geochronology. *Geoscience Frontiers* **9**, 1479–93.
- Villaseca C, Merino E, Oyarzun R, Orejana D, Pérez-Soba C and Chicharro E** (2014) Contrasting chemical and isotopic signatures from Neoproterozoic metasedimentary rocks in the Central Iberian Zone (Spain) of pre-Variscan Europe: implications for terrane analysis and Early Ordovician magmatic belts. *Precambrian Research* **245**, 131–45.
- Watson EB and Harrison TM** (1983) Zircon saturation revisited: temperature and composition effects in a variety of crustal magma types. *Earth and Planetary Science Letters* **64**, 295–304.
- Watson EB, Wark DA and Thomas JB** (2006) Crystallization thermometers for zircon and rutile. *Contributions to Mineralogy and Petrology* **151**, 413–33.
- Winchester JA and Floyd PA** (1977) Geochemical discrimination of different magma series and their differentiation products using immobile elements. *Chemical Geology* **20**, 325–43.
- Yang AY, Langmuir CH, Cai Y, Michael P, Goldstein SL and Chen Z** (2021) A subduction influence on ocean ridge basalts outside the Pacific subduction shield. *Nature Communications* **12**, 1–10.
- Zavala-Monsiváis A, Barboza-Gudiño JR, Velasco-Tapia F and García-Arreola ME** (2012) Jurassic volcanic succession in the Charcas area, San Luis Potosí: contribution to understanding the Nazas Arc in northeastern Mexico. *Boletín de la Sociedad Geológica Mexicana* **64**, 277–93.
- Zellmer GF, Pistone M, Iizuka Y, Andrews BJ, Gómez-Tuena A, Straub SM and Cottrell E** (2016) Petrogenesis of antecryst-bearing arc basalts from the Trans-Mexican Volcanic Belt: insights into along-arc variations in magma-mush ponding depths, H₂O contents, and surface heat flux. *American Mineralogist* **101**, 2405–22.
- Zepeda-Martínez M, Martini M, Solari LA and Mendoza-Rosales CC** (2021) Reconstructing the tectono-sedimentary evolution of the Early–Middle Jurassic Tlaxiaco Basin in southern Mexico: new insights into the crustal attenuation history of southern North America during Pangea breakup. *Geosphere* **17**, 1294–317.
- Zhong S, Zhang N, Li ZX and Roberts JH** (2007) Supercontinent cycles, true polar wander, and very long-wavelength mantle convection. *Earth and Planetary Science Letters* **261**, 551–64.